Atmos. Chem. Phys. Discuss., 10, 27967–28015, 2010
www.atmos-chem-phys-discuss.net/10/27967/2010/
doi:10.5194/acpd-10-27967-2010

Atmospheric Chemistry and Physics Discussions

An accuracy assessment of the CALIOP/CALIPSO version 2 aerosol extinction product based on a detailed multi-sensor, multi-platform case study

M. Kacenelenbogen[1], M. A. Vaughan[2], J. Redemann[3], R. M. Hoff[4], R. R. Rogers[2], R. A. Ferrare[2], P. B. Russell[5], C. A. Hostetler[2], J. W. Hair[2], and B. N. Holben[6]

[1]ORAU/ NASA Ames Research Center, Moffett Field, CA, USA
[2]NASA Langley Research Center, Hampton, VA, USA
[3]Bay Area Environmental Research Institute, Sonoma, CA, USA
[4]Joint Center for Earth Systems Technology (JCET)/Goddard Earth Science and Technology Center (GEST), University of Baltimore County, MA, USA
[5]NASA Ames Research Center, Moffett Field, CA, USA
[6]NASA Goddard Space Flight Center, Greenbelt, MA, USA

Received: 13 July 2010 – Accepted: 29 October 2010 – Published: 16 November 2010

Correspondence to: Meloe Kacenelenbogen (meloe.s.kacenelenbogen@nasa.gov)

Published by Copernicus Publications on behalf of the European Geosciences Union.

Abstract

The Cloud Aerosol LIdar with Orthogonal Polarization (CALIOP), on board the CALIPSO platform, has measured profiles of total attenuated backscatter coefficient (level 1 products) since June 2006. CALIOP's level 2 products, such as the aerosol backscatter and extinction coefficient profiles, are retrieved using a complex succession of automated algorithms. The goal of this study is to help identify potential shortcomings in the CALIOP version 2 level 2 aerosol extinction product and to illustrate some of the motivation for the changes that will be introduced in the next version of CALIOP data (version 3, currently being processed). As a first step, we compared CALIOP version 2-derived AOD with the collocated MODerate Imaging Spectroradiometer (MODIS) AOD retrievals over the Continental United States. The best statistical agreement between those two quantities was found over the Eastern part of the United States with, nonetheless, a weak correlation (R ~0.4) and an apparent CALIOP version 2 underestimation (by ~66 %) of MODIS AOD. To help quantify the potential factors contributing to the uncertainty of the CALIOP aerosol extinction retrieval, we then focused on a one-day, multi-instrument, multiplatform comparison study during the CALIPSO and Twilight Zone (CATZ) validation campaign on August 04, 2007. This case study illustrates the following potential reasons for a bias in the CALIOP AOD: (i) CALIOP's low signal-to-noise ratio (SNR) leading to the misclassification and/or lack of aerosol layer identification, especially close to the Earth's surface; (ii) the cloud contamination of CALIOP version 2 aerosol backscatter and extinction profiles; (iii) potentially erroneous assumptions of the backscatter-to-extinction ratio (S_a) used in CALIOP's extinction retrievals; and (iv) calibration coefficient biases in the CALIOP daytime attenuated backscatter coefficient profiles.

ACPD
10, 27967–28015, 2010

1 Introduction

The Cloud Aerosol LIdar with Orthogonal Polarization (CALIOP), on board the CALIPSO platform (flying as part of the A-Train satellite constellation since April 2006), is a three-channel elastic backscatter lidar optimized for aerosol and cloud profiling. CALIOP measures high-resolution (1/3 km in the horizontal and 30 m in the vertical in low and middle troposphere) profiles of the attenuated backscatter by aerosols and clouds at visible (532 nm) and near-infrared (1064 nm) wavelengths along with polarized backscatter in the visible channel (Winker et al., 2009). These data are distributed as part of the level 1 CALIOP products. The level 2 CALIOP products are derived from the level 1 measurements using a complex and intricate succession of algorithms that are described in detail in a special issue of the Journal of Atmospheric and Oceanic Technology (e.g., Winker et al., 2009). The level 2 retrieval scheme is composed of a feature detection scheme, a module that classifies features according to layer type (e.g., cloud vs. aerosol) and sub-type, and, finally, an extinction retrieval algorithm that estimates the aerosol backscatter, the extinction coefficient profile and total column aerosol optical depth (AOD) for an assumed extinction-to-backscatter ratio (also called S_a) for each detected aerosol layer.

For a select list of observables, CALIOP attenuated backscatter, aerosol backscatter and extinction coefficient profiles have been shown to yield reasonable agreement with ground-based (Kim et al., 2008; Mamouri et al., 2009; Mona et al., 2009; Pappalardo et al., 2010) and airborne lidar measurements (McGill et al., 2007; Omar et al., 2009; Rogers et al., 2010). For example, Pappalardo et al. (2010) have observed a mean percentage difference of less than 20% between level 1 CALIOP and ground-based EARLINET (European Aerosol Research Lidar Network) lidar measurements of attenuated backscatter profiles since June 2006 over Europe, showing an absence of evident biases in the CALIOP raw signals. Rogers et al. (2010) have conducted the most extensive quantitative assessment study of the CALIOP 532 nm total attenuated backscatter to-date, using coincident data from 86 underflights by the NASA-Langley High Spectral

ACPD
10, 27967–28015, 2010

Resolution Lidar (HSRL) (Hair et al., 2008) acquired since June 2006. Results show HSRL and CALIOP (version 2) 532 nm total attenuated backscatter agree within 1.1% ±23% for daytime lighting conditions in the free troposphere. Kim et al. (2008) showed that CALIOP, when compared to a ground-based lidar in Korea, has detected cloud and aerosol top/base layers and retrieved the aerosol extinction profiles correctly within respectively 0.10 km and 30% in cloud-free nighttime and semi-transparent cirrus cloud conditions. According to Omar et al. (2009), CALIOP (Version 2) generally overestimates the HSRL extinction measurements for several case studies, with an average extinction bias of 0.003 km^{-1} (~24%) during the CALIPSO and Twilight Zone (CATZ) validation campaign and 0.015 km^{-1} (~59%) during the Gulf of Mexico Atmospheric Composition and Climate Study (GoMACCS).

Nonetheless, there are significant uncertainties associated with the version 2 CALIOP aerosol extinction and backscatter retrievals, and these are not well-quantified in any ancillary quality assurance information included in the level 2 data files. These uncertainties are introduced by several different factors that are often related to each other (Winker et al., 2009; Yu et al., 2010). First of all, the CALIOP layer detection scheme will most likely fail to detect layers with aerosol backscatter coefficients falling below a sensitivity threshold of $2\sim4 \times 10^{-4}$ km^{-1} sr^{-1} in the troposphere (Winker et al., 2009). Consequently, if we assume a lidar extinction-to-backscatter ratio (S_a) of 50 sr, the minimum detectable extinction coefficient is in the neighborhood of 0.01 to 0.02 km^{-1} (corresponding to a lowest detectable AOD of 0.02–0.04 in a homogenous 2 km planetary boundary layer). A second significant source of error is the lack of photons returned from underneath highly attenuating layers, such as dense aerosol and cloud layers. This may result in the erroneous or total lack of aerosol identification in the lower part of a given profile. In such situations, the CALIOP detection algorithm can incorrectly identify the lower portions of an aerosol layer as being clear air, and thus no aerosol extinction coefficients will be reported for these regions. A third factor impacting the CALIOP extinction retrieval is the occasional misclassification of layer type. Aerosols can be misclassified as clouds, and vice versa (Liu et al., 2009). Classification

ACPD
10, 27967–28015, 2010

errors can also occur in the aerosol subtyping algorithm (Omar et al., 2009), leading to an incorrect assumption about the appropriate extinction-to-backscatter ratio. The CALIOP AOD fractional error is similar to the S_a fractional error for small AOD values (Winker et al., 2009). On the other hand, as the AOD increases, the AOD fractional error will quickly become much higher than the S_a fractional error. For example, a fractional error of 30% for S_a would result in an AOD fractional error of ~50% for an AOD of 0.5 and nearly 100% for an AOD of 1.

Despite these uncertainties, there have been a number of publications using CALIOP version 2 level 2 data in a qualitative or even quantitative manner. Focusing on articles published in 2010, some authors recognize the largely unvalidated nature of level 2 version 2 data. Among those, there have been attempts to produce more accurate CALIOP data by applying further cloud-screening (Sekiyama et al., 2010) or even an intensive data screening scheme (Yu et al., 2010). Some mention the uncertainties associated with the level 2 version 2 data but apply no specific filtering (e.g., Peyridieu et al., 2010; Jones et al., 2009). We note that many articles in 2010 (and probably a few more in the previous years) omit discussions on the accuracy of level 2 version 2 CALIOP data. This is, for example, the case for Gonzi et al. (2010), who qualitatively compared biomass burning injection height estimates from the GEOS-Chem model to unfiltered CALIOP vertical feature mask data. This latter product is also used to suggest the presence of an extended aerosol layer over central India that could be associated with agriculture crop residue burning activities (Sharma et al., 2010), and to help determine the altitude of smoke plumes over the US during Summer 2006 (McMillan et al., 2010). Finally, Kuhlmann et al. (2010) make more intensive use of the unfiltered level 2 CALIOP aerosol layer product to draw conclusions regarding the particle type and general aerosol vertical distribution during the Asian summer Monsoon. The conclusions drawn in these works are not necessarily wrong, and, in fact, may be absolutely correct. However, it is difficult to embrace the results reported, simply because the data from which they are derived are not yet well validated.

ACPD
10, 27967–28015, 2010

In this study we attempt to assess the consistency between the CALIOP AOD retrievals and comparative aerosol observations from multiple sources and platforms (including ground-based, airborne and satellite instruments). As a first step, we compare MODIS (MODerate Imaging Spectroradiometer, collection 5) and CALIOP total column AOD over the United States for a period of four months during the summer of 2007 in an attempt to assess the general consistency between the two satellite instruments. Let us point out that Levy et al. (2010) demonstrate the global validation of total MODIS AOD over dark-land targets with more than 66% of MODIS AOD matching those of the AErosol RObotic NETwork (AERONET, Level 2 measurements at over 300 sites) within the expected uncertainty defined by $\Delta AOD = \pm 0.05 \pm 0.15$ AOD. We find a general underestimate of the MODIS-derived AOD by CALIOP and discuss possible explanations for the observed discrepancies in Sect. 3. In Sect. 4, we then focus on a one-day, multi-sensor case study that yielded AOD differences similar to the mean differences found in our broader MODIS-CALIOP comparison. This case study was part of the nine ground-based CATZ field campaigns (each campaign occurring on separate days between 26 June and 29 August 2007) in Virginia and Maryland, when four AERONET sites were deployed and the NASA Langley Research Center airborne HSRL was flown along the daytime CALIOP track, with coincident space-borne observations available from MODIS and POLDER (Polarization and Directionality of Earth's Reflectances). The detailed suborbital observations, and in particular, the comparison of coincident CALIOP and HSRL profiles, are used to explore the following potential reasons for the overall bias between the MODIS AOD and the CALIOP version 2 AOD product: (i) CALIOP's low Signal to Noise Ratio (SNR) which can lead to the misclassification and/or lack of aerosol layer identification, especially close to the Earth's surface; (ii) the cloud contamination of CALIOP aerosol backscatter and extinction profiles; (iii) a potentially erroneous S_a assumption in CALIOP's extinction retrieval and (iv) calibration errors in the CALIOP daytime attenuated backscatter coefficient profiles.

Our study is intended to help identify potential shortcomings in the Version 2 level 2 aerosol extinction product and to illustrate some of the motivation for the changes that

ACPD
10, 27967–28015, 2010

are being introduced in the next version of CALIOP data (Version 3, released in May 2010). Based on the multi-instrument, multi-platform comparison study, we seek to quantify the major factors contributing to the uncertainty of the CALIOP aerosol extinction retrieval. We submit that the identification and discussion of retrieval uncertainties provided here will help understand and interpret the results obtained in previous studies like the ones cited above.

2 Instruments

2.1 Aeronet

The AErosol RObotic NETwork (AERONET) (Holben et al., 1998) is composed of automatic sun-sky scanning spectral radiometers. The AOD and Ångström exponent (called Å, expresses the wavelength dependence, λ, of the AOD and is defined as the slope of the first order linear regression of log(AOD) versus log(λ)) are determined by direct sun measurements. The aerosol size distribution and optical parameters (such as the single scattering albedo, volume concentration, refractive index, etc.) are derived from the angular distribution of sky radiances measured in the almucantar according to the algorithm developed by Dubovik and King (2000a). In this study, we use version 2-level 1.5 AERONET data (Smirnov et al., 2002). During the CATZ field experiment, the AERONET sunphotometer observations were sampled more frequently than in the case of the standard automatic mode measurement protocol (Holben et al., 1998), preventing the data from being labeled level 2. However, the correct calibration of the sunphotometers during the experiment results in the same estimated total uncertainty in the direct AOD measurements as for the level 2 data: ~0.010–0.021 (Eck et al., 1999). In the case of AOD values above 0.2 at 440 nm, Dubovik et al. (2000b) reports accuracies of 0.03 for the single scattering albedo, 0.02–0.04 for the real part of the refractive index, 30% (50%) of the imaginary part of the refractive index in case of low (high) absorption, 15–35% (15–100%) of the volume size distribution in case of a

ACPD
10, 27967–28015, 2010

radius between 0.1 and 7 µm (lower than 0.1 µm or above 7 µm). In the case of lower AOD values (AOD(440)≤0.2), the accuracy levels drop down to 0.05–0.07 for SSA, 80%–100% for the imaginary part of the refractive index, and 0.05 for the real part of the refractive index.

2.2 CALIOP

CALIOP on the CALIPSO platform employs a linearly polarized laser that transmits pulses at 532 nm and 1064 nm. The two 532 nm receiver channels separately measure the components of the 532 nm backscatter signal polarized parallel and perpendicular to the outgoing beam. The measured CALIOP attenuated backscatter coefficient at wavelength λ and range z, $\beta'_{\lambda}(z)$, can be written as:

$$\beta'_{\lambda}(z) = (\beta_{a,\lambda}(z) + \beta_{m,\lambda}(z))T^2_{\lambda}(z) \quad (1)$$

where $\beta_{a,\lambda}$ and $\beta_{m,\lambda}$ are, respectively, the aerosol and molecular retrieved backscatter coefficient profile, and $T^2_{\lambda} = T^2_{a,\lambda}T^2_{m,\lambda}T^2_{O_3,\lambda}$ is the atmospheric two-way transmittance (i.e., signal attenuation) due to aerosols, molecular scattering, and absorbing gases such as ozone.

The aerosol transmittance between the lidar calibration region and range z, $T_{a,\lambda}(z)$, can be expressed as follows:

$$T^2_{a,\lambda}(z) = \exp\left(-2\int_{z_0}^{z}\alpha_{a,\lambda}(z)dz\right) = \exp(-2\tau_{a,\lambda}) \quad (2)$$

where z_0 is the height of the calibration region, $\alpha_{a,\lambda}$ is the aerosol extinction coefficient and $\tau_{a,\lambda}$, the aerosol optical depth.

We will be concentrating mostly on the CALIOP-measured total attenuated backscatter coefficients, $\beta'_{532}(z)$, the retrieved aerosol backscatter coefficients, $\beta_{a,532}(z)$, and

ACPD
10, 27967–28015, 2010

the retrieved aerosol extinction coefficient profiles, $\alpha_{a,532}(z)$ along the CALIOP ground track.

The extinction coefficient profiles are retrieved using a globally automated feature recognition algorithm that assumes a range-invariant extinction-to-backscatter ratio, also referred to as lidar ratio ($S_{a,532} = \alpha_{a,532}(z)/\beta_{a,532}(z)$) for each layer detected. The CALIOP value of S_{a532} used for any layer depends on the geographical location, the integrated attenuated backscatter color ratio, the layer-integrated volume depolarization ratio, and a general Look Up Table (LUT) (Liu et al., 2009; Omar et al., 2009). The prelaunch goal of the CALIPSO mission was to retrieve aerosol extinction coefficients accurate to within ±40% (Winker et al., 2003). We have attributed names to all the CALIOP parameters used in this study. They are listed in Table 1 along with the standard variables, original file name, level, and spatial resolution due to averaging.

CALIOP's version 2 data products do not provide uncertainty estimates for retrieved optical parameters such as AOD and extinction coefficients. The uncertainties attributed to the CALIOP aerosol optical depths can be obtained by applying an error estimator algorithm to the quantities reported in the aerosol layer products, taking into account the relative error on the lidar ratio, the calibration coefficient and the SNR for each detected aerosol layer. The error on the SNR may be slightly more complex to estimate as it depends on the backscatter intensity, the lighting conditions (i.e., day vs. night), and the amount of horizontal averaging applied to the initial attenuated backscatter profiles.

2.3 HSRL

Retrieval of aerosol extinction profiles using the standard elastic backscatter lidar technique requires either a measurement of AOD to constrain the extinction retrieval (Young, 1995; McGill et al., 2003) or an assumption on the aerosol extinction-to-backscatter ratio value (Cattrall et al., 2005). On the other hand, the HSRL technique directly measures the vertical profile of aerosol extinction and extinction-to-backscatter ratio, without requiring ancillary aerosol measurements or assumptions about aerosol

ACPD
10, 27967–28015, 2010

type (Hair et al., 2008). The HSRL technique is typically employed for the 532 nm wavelength utilizing the iodine vapor filter technique (Hair et al., 2001, 2008; Piironen et al., 1994). The received 532 nm backscatter return is split between three optical channels: (1) one measuring the backscatter (predominantly aerosol) polarized orthogonally to the transmitted polarization, (2) one measuring 10% of the molecular and aerosol backscatter polarized parallel to the transmitted polarization, and (3) one passing through an iodine vapor cell which absorbs the central portion of the backscatter spectrum, including all of the Mie backscatter, and transmits only the Doppler/pressure-broadened molecular backscatter. This third channel, (the "molecular channel") is used to retrieve the extinction profile and all three channels are used to retrieve profiles of aerosol backscatter and extinction coefficients and aerosol depolarization ratios. Hair et al. (2008) described the potential errors introduced in any of these quantities and found the 532 nm extinction systematic errors to be less than 0.01 km^{-1} for typical aerosol loading. Table 2 describes the HSRL analyzed data products used in this study. We use an HSRL subset file with a ~4/3 km horizontal and 30 m vertical resolution. The ~4/3 km horizontal resolution of the HSRL aerosol backscatter (e.g. extinction and lidar ratio) coefficient profiles is obtained by computing 10 (e.g. 60) second running averages of the raw data (initially sampled at 2 Hz), then decimating the results by a factor of 20.

2.4 POLDER and MODIS

POLDER-3 (POLarization and Directionality of Earth's Reflectances, 3rd version of the instrument, on board the PARASOL platform) and MODIS (on board the Earth Observing System (EOS) AQUA satellite) are both passive radiometers, with both platforms being simultaneously part of the A-Train during five years (December 2004–2009), including our study period of Summer 2007. POLDER's strength is the measurement of directional and polarized characteristics of the solar radiation reflected by the Earth-Atmosphere system. MODIS, on the other hand, has a finer spatial and spectral resolution. POLDER AOD estimates of polarizing particles over land surfaces are retrieved in

ACPD
10, 27967–28015, 2010

the 865 nm channel. MODIS AOD is retrieved over oceans in 7 different spectral bands (6 + extrapolated) from the visible to the near infrared and over land in 3 bands (2 + 1 interpolated). POLDER's spatial resolution is 5 × 6.5 km (500 × 500 m for MODIS) and its wide field of view induces a 1600 km swath (2330 km for MODIS) that allows a nearly global daily coverage. To increase the signal to noise ratio, the standard retrieval algorithm is applied to 3 × 3 POLDER pixels (20 × 20 for MODIS), leading to a resolution in the aerosol AOD of 15 × 19.5 km (10 × 10 km for MODIS). The AOD retrieval from the POLDER polarized measurements is described by Deuzé et al. (2001) and the MODIS AOD retrieval algorithm over land is described in Kaufmann and Tanré (1998). The polarization by aerosols mainly comes from small spherical particles in the accumulation mode (Vermeulen et al., 2000), indicating that POLDER-derived AOD is well suited for remote sensing of fine mode particles. Validation studies suggest that the expected uncertainty on the MODIS AOD over dark land surfaces could be represented by $\Delta\text{AOD} = \pm 0.05 \pm 0.15\,\text{AOD}$ (Levy et al., 2010).

3 Evaluation of Version 2 CALIOP extinction retrieval: summer 2007

In this study, for convenience, all satellite data are remapped on the 12 × 12 km Community Multiscale Air Quality (CMAQ) model grid (US EPA, 1999). Each MODIS 10 × 10 km cell center has been attributed to the closest CMAQ cell center. In the case of CALIOP, the product to be remapped is the standard level 2 extinction coefficient, $\alpha_{a,532}$@40 km (see Table 1). CALIOP provides one constant extinction vertical profile between start-location l_{start} and end-location l_{end}, with a horizontal distance of 40 km between l_{start} and l_{end}. In addition, each $\alpha_{a,532}$@40 km profile is separated from adjacent profiles by a distance of 1/3 km along the CALIOP track. A 12 × 12 km CMAQ cell can then contain, at the most, two different parts of $\alpha_{a,532}$@40 km profiles. When the CMAQ cell contains only one $\alpha_{a,532}$@40 km profile, this profile is simply attributed to the cell's center; on the other hand, when the cell contains two different $\alpha_{a,532}$@40 km profiles, the final profile attributed to the cell's center is an average of those two

ACPD
10, 27967–28015, 2010

$\alpha_{a,532}$@40 km profiles weighted by the number of corresponding β'_{532}@1/3 km profiles contained in the cell. The CALIOP AOD data value for each cell is then obtained by integrating its corresponding $\alpha_{a,532}$@40 km profile on the vertical.

We start this study by comparing MODIS and CALIOP AOD values over the continental United States from June to September 2007. Multiple constraints have been applied to the data sets for this study. First of all, we have kept only positive MODIS AOD and CALIOP $\alpha_{a,532}$@40 km values. Secondly, for rigorous cloud-clearing and the elimination of outliers, the CALIOP $\beta_{a,532}$@40 km data are required to be below 0.011 sr^{-1} km^{-1} (a value typically found for a polluted continental or biomass burning type of aerosol with an extinction-to-backscatter lidar ratio of 70 sr and an $\alpha_{a,532}$@40 km value of 0.8 km^{-1}, corresponding to a visibility of >~5 km). Finally, CALIOP AOD values are computed only when aerosol is detected in 20 or more vertical bins within a 40- km averaged profile. According to Table 1, the vertical resolution of the CALIOP $\alpha_{a,532}$@40 km product is 120 m (below 8 km). Hence, the 20-bin requirement on the vertical translates into a minimum layer thickness of 2.4 km, assuming these points are consecutive within a profile.

Figure 1 shows the MODIS-CALIOP AOD comparison over the entire United States (on the left) and over the Eastern part of the US (on the right, longitude above −100°). Each data set has been arranged in twenty different MODIS and CALIOP AOD bins. Figure 1 shows the corresponding data count for each bin center. The red lines on Fig. 1a and b show the first principal component regression (Kendall, 1957) that fits a line by minimizing MODIS and CALIOP AOD residuals simultaneously while giving both data sets equal weight.

According to Fig. 1, the statistical agreement between MODIS and CALIOP AOD is slightly better over the Eastern part of the United States (right), where 807 samples have a correlation coefficient of 0.43, a slope of 0.34, an offset of 0.17 and a root-mean-squared-deviation of 0.26. Discrepancies between MODIS AOD retrievals in the Western and Eastern part of the United States could come from uncertainties in the MODIS cloud masking of low stratus clouds (more often observed in the West) but

ACPD
10, 27967–28015, 2010

also from different terrain and different model surface reflectivity assumptions. A large number of collocated CALIOP and MODIS AOD values are below 0.25 in both Fig. 1a and b (respectively 42% and 36%). Among those values, Fig. 1b indicates a slightly greater averaged CALIOP AOD value (0.15) compared to MODIS (0.12). For example, 45 data points show a MODIS AOD in the [0.10–0.20] range with a corresponding CALIOP AOD between 0.19 and 0.25.

The general underestimation (by 66%) of the standard version 2 CALIOP extinction product ($\alpha_{a,532}$@40 km) is demonstrated by the slope of the regression line between CALIOP and MODIS AOD on Fig. 1b. Although similar results have been shown in science team (Redemann et al., 2009) and conference proceedings (Kittaka et al., 2008), the authors do not know of any comparison study between CALIOP and MODIS AOD that has already been reported in the peer reviewed literature.

On one hand, the discrepancies between the CALIOP and MODIS AOD data sets in Fig. 1 could be explained by the uncertainties in the MODIS AOD retrieval. Indeed, Kaufman and Tanré (1998) and Chu et al. (2002) report errors in the MODIS AOD due to wrong correction of the surface reflectance (5–20%), instrument calibration (2–5%), cloud-screening (0–10%), and aerosol model (10–20%). On the other hand, there are numerous reasons for the CALIOP AOD to be biased as well: wrong assumptions on the extinction-to-backscatter lidar ratio, bias in the cloud-screening of the profiles, inadequate detection of tenuous aerosol layers during daytime due to a low SNR and/or a lack of photons reaching the surface, especially, after going through thick aerosol plumes. Let us mention that the overall CALIOP underestimation of the MODIS AOD on Fig. 1 does not concur with the general CALIOP overestimation of the HSRL extinction coefficients by ~20% during the CATZ experiment in Omar et al. (2009). The latter was found to be largely due to a CALIOP overestimation of the HSRL extinction-to-backscatter lidar ratios by about 7.4 sr (~20%).

In order to understand and illustrate some of the potential reasons for discrepancies between the MODIS and CALIOP AODs, in the following section, we explore a carefully selected case study. This case study features collocated ground-based sunphotometer

ACPD
10, 27967–28015, 2010

and air-borne lidar observations during the CATZ field campaign and yields MODIS-CALIOP AOD differences that are representative of the larger data set explored in Fig. 1.

4 Evaluation of Version 2 CALIOP extinction retrieval: 4 August 2007 (a CATZ case study)

4.1 Aerosol type and sources

The MODIS true color RGB image in Fig. 2a shows some haze hovering over a significant part of the Mid-Atlantic East Coast of the United States, extending from Virginia to New Jersey on 04 August 2007. This particle plume is most likely a mix of aerosol pollution from regional anthropogenic sources and smoke coming from wildfires in the Northwestern United States. According to the National Interagency Fire Center, more than a dozen large fires were reported from late July to early August of 2007 in the Northern Rockies of Idaho and Montana. By 7 August, those fires had affected nearly 400 000 acres in Idaho and had produced smoke that blanketed much of the United States. The 3 day-HYSPLIT air mass back-trajectories at three different heights from 500 to 1500 m (Draxler et al., 2010; Rolph, 2010) (Fig. 2a), suggests that a part of the aerosol plume over the East Coast on 4 August 2007 may have come from the Northern part of the United States.

We will be focusing our study over the CATZ-Sanders Elementary School AERONET station (39.04 N; −77.51 W), one of the four sunphotometer sites that were deployed along the CALIOP track during the CATZ campaign. This station, shown by a white diamond on Fig. 2a, will hereafter be called “CATZ-Sanders”. CATZ-Sanders was roughly 138 m away from the CALIOP track and the overpass on 04 August occurred at 18:27 UTC. Aerosol microphysical and optical properties derived from the inversion of two angular sky-radiance measurements at CATZ-Sanders on 4 August 2007 are shown in Fig. 2b.

ACPD
10, 27967–28015, 2010

The aerosol plume over CATZ-Sanders seems predominantly composed of fine particles, with Ångström coefficients (Å between 440–870 nm) of 1.92 (Fig. 2b). This is confirmed by the volume size distributions that show, for both measurements, a peak around 0.16 µm in radius. Finally, the particles show significant light absorption with a single scattering albedo coefficient (ω_0) between 0.94 and 0.96 and an imaginary part of the refractive index (Im(η)) of about 0.01.

4.2 Ground-based, airborne and space-borne AOD measurements

Fig. 3a shows the locations of CATZ-Sanders (white diamond), the CALIOP ground track along the closest 40 km segment (white line), the corresponding airborne HSRL track segment (green line) and the closest CMAQ 12 x 12 km cell (red box). Recall that all satellite data are remapped onto the CMAQ grid and the closest CMAQ cell to CATZ-Sanders (red box on Fig. 3a) contains a remapped MODIS and CALIOP AOD observation. On the other hand, the closest CMAQ cell with available POLDER AOD data on 4 August 2007 is shown as a black box in Fig. 3a, at a distance of ~18 km between CATZ-Sanders and the closest POLDER extinction observation. Table 3 sums up the horizontal distances between each measurement during the experiment.

Figure 3b shows the collocated ground-based (sunphotometer, black), airborne (HSRL, orange) and space-borne (MODIS green, POLDER red and CALIOP blue) AOD observations. The sunphotometer is the only instrument providing a full temporal evolution of AOD values throughout the afternoon and evening of 04 August 2007. The HSRL instrument completes this temporal information with two overpasses over CATZ-Sanders around 16:48 and 17:52 UTC.

It should be noted that HSRL overflew CATZ-Sanders ~30 min earlier (17:52 UTC compared to 18:27 UTC for CALIOP) and ~900 m away from the CALIOP ground-track (Table 3). A ground-based wind profiler instrument in Beltsville (Maryland) shows an average wind speed of ~2.6 m per second from the surface up to ~3.8 km between the HSRL and CALIOP overpass time, blowing mainly from the northwest. Accordingly, a 30-min air mass travel time between the HSRL and CALIOP observations would

ACPD
10, 27967–28015, 2010

represent a distance of roughly 5 km at the ground. Whether it is statistically relevant to compare aerosol extinction profiles and AOD retrievals on that time and horizontal scale is difficult to ascertain. According to Fig. 3b, there is a fair amount of variation in the AERONET AOD measurements throughout the afternoon and evening of 4 August 2007 (from 0.48 to 0.87 at 532 nm). The variation $\pm 1/2$ h around the time of the A-Train overpass is smaller but still significant, with AOD values (at 532 nm) ranging from 0.48 to 0.73. This variation, similar to the range of AOD $\pm 1/2$ h preceding the A-Train overpass, corresponds to a change of ~35% in the AOD (0.25 compared to 0.71 at the A-train overpass time) over a course of ~5 km (distance covered by the air mass in $\pm 1/2$ h with an averaged wind speed of ~2.6 m/s). Autocorrelation analysis of in situ optical measurements have shown a correlation of $R = 0.9$ for time and space offsets of less than ~3 h and 60 km ($R = 0.8$ for time and space offsets less than ~6 h and 120 km) (Anderson et al., 2003). In other words, Anderson et al. (2003) demonstrate that on scales larger than a few hours or a few tens of kilometers, aerosols cannot be considered as homogeneous in space and time, when measured at one local point. In addition, Redemann et al. (2006) show small instrumental noise and also small natural variability of AOD retrieved by the NASA Ames Airborne Tracking Sunphotometer, AATS-14, on a horizontal scale of 15 km during the Extended-MODIS-λ Validation Experiment (EVE) campaign in April of 2004 (all AATS derived AOD yield auto-correlations of 0.96). To those studies should be added the effect of vertical mixing, which could either decrease or increase variability in remotely sensed total column AOD observations. The guidance for the CALIOP validation plan using ground-based lidar (http://calipsovalidation.hamptonu.edu) is that both CALIOP and ground instruments have to be within a horizontal radius of 100 km. Nonetheless, the spatial variability of aerosols and their extinction properties vary from one environment to another. Shinozuka et al. (2010) have shown a ~20% variation of the AOD over the course of 30 km when flying the NASA Ames Airborne Tracking Sunphotometer (AATS-14) through a biomass burning plume over Canada during the ARCTAS field campaign (Arctic Research of the Composition of the Troposphere from Aircraft and Satellites).

ACPD
10, 27967–28015, 2010

On another hand, the AOD was shown to vary only by ∼3% during another phase of the same campaign over Alaska.

The HSRL AOD retrieval (0.52) is lower than the AERONET direct sun AOD measurement (0.57) by 0.05 at the time of the second HSRL overpass (∼18:00 UTC). The AERONET level 1.5 measurements could be contaminated by thin cirrus clouds, not observed by the downward pointing HSRL instrument, flying at an altitude of ∼9 km. CALIOP's perpendicular (532 nm) and total attenuated backscatter (1064 and 532 nm) curtain scenes show no particular evidence of depolarizing cirrus crystals above the HSRL measurements but this could be due to CALIOP's low SNR, especially by day. The HSRL AOD measurement is only derived below ∼6.4 km, which may lead to a slight underestimation by the HSRL due to aerosol above ∼6.4 km. The distance of ∼900 m between both instruments (Table 3) may also lead to differences in AOD.

At the time of the A-train overpass, MODIS and AERONET report similar AOD retrieval values (with a difference of 0.04, below MODIS's AOD uncertainty of ∼0.15, 0.05 + 15% of 0.67). On the other hand, POLDER underestimates the AERONET AOD by 0.13. This slight difference could be due to uncertainties in the PARASOL inversion algorithm. Some bias could also be due to the satellite's coarse spatial resolution in a temporally and spatially varying aerosol field, especially for POLDER with a coarser resolution than MODIS and further away from the sunphotometer (Table 3). Let us also mention that POLDER is sensitive to fine polarizing particles over land and, thus, retrieves the fine mode AOD when MODIS retrieves the AOD corresponding to the entire volume size distribution of the particles (see Fig. 2b).

In conclusion, all three AOD observations (i.e., MODIS (0.67), PARASOL (0.58) and HSRL (0.52)) are contained in the AERONET AOD envelope within ±1/2 h around the A-Train overpass (0.48 to 0.73 at 532 nm). However, that is not the case for the CALIOP V2 AOD value (0.32), which is lower than all other AOD measurements in Fig. 3b, similar to the CALIOP-MODIS comparison in Fig. 1. In the following section, we investigate the potential reasons for a disagreement between the AOD calculated from CALIOP's version 2 extinction product and the rest of the AOD measurements in Fig. 3b.

ACPD
10, 27967–28015, 2010

4.3 HSRL and CALIOP backscatter and extinction coefficient profiles

Figure 4 shows the CALIOP and HSRL β'_{532} cross sections of attenuated backscatter (also called "curtain scene") along the 40 km segment of their ground tracks close to CATZ-Sanders (respectively corresponding to the white and green lines on Fig. 3a). Both CALIOP and HSRL are shown at a horizontal resolution of ~4/3 km (output resolution of the "subset" HSRL file and sliding average of four CALIOP β'_{532} @ 1/3 km profiles). A dashed black vertical line on all three Figures shows the closest profile to CATZ-Sanders on 4 August 2007.

The difference between the CALIOP "curtain scenes" shown in Fig. 4a and b reflects an additional cloud-screening of the data. Yost et al. (2008) compared MODIS images overlaid with the CALIOP cloud@1/3 km product (detected and reported at a 1/3 km resolution), and the feature@5 km product (detected at all resolutions and reported at 5 km). It was shown that the CALIOP 1/3- km detection results are entirely consistent with the MODIS image. However, in regions populated by broken boundary layer clouds, layers detected at coarser resolutions (1- km and above) are frequently misclassified as cloud. This was determined to be strictly a coding error in the cloud-clearing procedure, and not related to the algorithm design. To circumvent this error, in this part of our study, an additional cloud screening has been applied to all CALIOP β'_{532} @ 1/3 km profiles using the cloud@1/3 km product: all CALIOP β'_{532} @ 1/3 km coefficients are deleted underneath the highest detected cloud in the cloud@1/3 km product.

The black circle on Fig. 4a, b and c points out a region of the "curtain scene" showing strong initial raw β'_{532} @ 1/3 km coefficient values around 2.2 km on the vertical (Fig. 4a). This signal is classified as a cloud in the cloud@1/3 km product and is removed on Fig. 4b, thanks to the additional cloud screening described above. Figure 4c reports a lack of HSRL data in the corresponding region, most probably due to the presence of clouds as well (the HSRL data are cloud-screened, see Table 2).

Figure 4 illustrates the differences in the SNR of the HSRL and CALIOP instruments. The CALIOP "curtain scene" (Fig. 4b) appears much noisier than the HSRL cross

ACPD
10, 27967–28015, 2010

section (Fig. 4c), which makes it harder to analyze in terms of potential atmospheric vertical composition. On the other hand, Fig. 4c seems to show two fairly separate and spatially homogeneous stronger regions in the β'_{532} intensity on the vertical: the lowest one lies roughly between 1 and 2 km and the uppermost one is around 3 km. In addition, the closest point to CATZ-Sanders on the HSRL track (black dashed line on Fig. 4c) seems fairly representative of the rest of the 40 km "curtain scene".

Figure 5a shows the closest CALIOP and HSRL β'_{532} profile to CATZ-Sanders (black dashed line on Fig. 4b and c). Both CALIOP (Fig. 5a, blue) and HSRL (Fig. 5a, red) profiles are shown at a ~4/3 km resolution (output resolution of the HSRL subset file and selection of the closest CALIOP profile in the 4/3 km-resolution "curtain scene" of Fig. 4b). The CALIOP β'_{532} profile still clearly shows a low SNR compared to the HSRL β'_{532} profile.

CALIOP's low SNR (as shown on Figs. 4b and 5a), especially in daytime, requires the spatial averaging of the attenuated backscatter profile over a significant horizontal distance to detect potential features. This is one of the tasks of the Selective Iterated BoundarY Locator (SIBYL) in CALIOP's automated level 2 product routine (Vaughan et al., 2009). In short, SIBYL consists of an algorithm that iteratively averages profiles at different horizontal scales (5, 20 or 80 km), scans those averaged profiles to detect aerosol and cloud layers, and removes detected layers from the profiles before further averaging. As a result, strongly scattering layers and portions of layers are detected at finer spatial resolution, while more tenuous regions are detected at coarser resolutions. All layers detected are then classified according to type and subtype (Liu et al., 2009; Omar et al., 2009). Particulate backscatter and extinction coefficients are then derived for each layer detected at the 5-km, 20-km, and 80-km averaging interval, using profiles of $\beta'(z)$ averaged horizontally to the spatial resolution at which the layer was detected (Young and Vaughan, 2009). In CALIPSO's version 2 data products, the level 2 "native resolution" $\beta_{a,532}$ and $\alpha_{a,532}$ profiles are further averaged (layers detected at 5-km or 20-km) or replicated (80-km layers) as required to be reported at a uniform

ACPD
10, 27967–28015, 2010

final resolution of 40 km horizontal and 120 m vertical (Table 1).

The closest $\beta_{a,532}$@40 km profile to CATZ-Sanders is shown in Fig. 5b (black), along with the collocated HSRL $\beta_{a,532}$ profile (red). Unlike the processing of CALIOP profiles, we saw no necessity to average the HSRL profiles on a similar horizontal distance at the ground because of HSRL's considerably higher SNR and accuracy. Figure 4c supports this decision by showing a spatially uniform atmospheric "curtain scene" in the vicinity of CATZ-Sanders. In addition, the HSRL would cover 40 km in a few minutes (HSRL flies at ~117 m/s) compared to a few seconds for CALIOP (flies at ~7 km/s), adding potential temporal differences in the HSRL-CALIOP comparison.

In Fig. 5b, although the CALIOP $\beta_{a,532}$@40 km profile reports no aerosol above ~3.2 km or below ~1.4 km, both CALIOP $\beta_{a,532}$@40 km and HSRL $\beta_{a,532}$ profiles seem to show mostly two intensity peaks on the vertical. The change in intensity between the uppermost and the lowest peak could be due to either a change in the particle type (size and shape, hence different aerosol cross section and phase function) and/or a change in the particle concentration and does not necessarily show two separate aerosol layers on the vertical. Concerning the uppermost aerosol peak, the HSRL and CALIOP signals compare fairly well between 2.3 and 3.2 km. The standard CALIOP 5-km aerosol products (aerosol@5 km, Table 1) locate this layer (detected at a horizontal averaging of 20 km) between 2.7 and 3.1 km, and define it as polluted dust aerosol particles (CALIOP model $S_a = 65$ sr). The lowest intensity peak consists of a fairly constant portion of the HSRL $\beta_{a,532}$ profile recording roughly 0.003 km^{-1} sr^{-1} from the lowest few hundred meters close to the ground up to 1.9 km. Although the corresponding CALIOP profile starts around 1.4 km and misses a lot of the aerosol signal observed by the HSRL, it seems to pick up the lowest peak with an overestimation of 1×10^{-3} km^{-1} sr^{-1} at 1.9 km before a maximum of 5.9×10^{-3} sr^{-1} km^{-1} at 2.2 km. The standard CALIOP 5-km aerosol products define the lowest aerosol layer (detected with a horizontal averaging of 80 km) as being located between 1.5 and 2.5 km, and composed of dust aerosol particles (CALIOP model $S_a = 40$ sr). The presence of either polluted dust or pure dust aerosol particles is highly unlikely according to the findings

ACPD
10, 27967–28015, 2010

of Sect. 4.1. Indeed, the optical and microphysical properties of the aerosol plume over CATZ-Sanders tend to show a predominance of fine and strong light absorbing particles, possibly coming from a mix of haze and biomass burning particles.

In summary, Fig. 5b shows fairly good agreement between the HSRL $\beta_{a,532}$ and CALIOP $\beta_{a,532}$@40 km profiles, except for a lack of CALIOP values below ~1.4 km and a strong peak in the CALIOP $\beta_{a,532}$ signal around 2.2 km. The immediate reasons could be that (i) CALIOP, with its low SNR, cannot detect tenuous aerosol layers or reach all the way down to the lidar-detected surface due to aerosol attenuation and ii) there is a significant bug in the cloud-screening algorithm, that could explain the disparity between CALIOP and HSRL $\beta_{a,532}$ around 2.2 km (corresponding to the height at which a cloud is reported in Fig. 4a).

Figure 5c compares the CALIOP $S_{a,532}$@40 km profile (=$\alpha_{a,532}$@40 km/$\beta_{a,532}$@40 km, Table 1) with the measured HSRL $S_{a,532}$ profile (see Table 2). For HSRL, $S_{a,532}(z)$ is simply the ratio of $\alpha_{a,532}(z)$ and $\beta_{a,532}(z)$, where both quantities are measured directly by the instrument. The CALIOP retrieval algorithm does not assume a profile of S_a values but assumes, instead, a single S_a value for each detected aerosol layer on the vertical. The fact that the $S_{a,532}$@40 km profile on Fig. 5c varies on the vertical is due to the averaging of different types of aerosols that were detected at different horizontal scales. Although CALIOP and HSRL show similar averaged S_a values in the vertical (66 sr for CALIOP compared to 64 sr for the HSRL), CALIOP shows a much smaller range of $S_{a,532}$@40 km (from 56 to 70 sr) compared to the HSRL (from 29 to 83 sr). The reason is that the variety of different S_a value assumptions in the CALIOP automated algorithm is much smaller than in reality. This observation leads to the introduction of a third potential explanation in the discrepancies between CALIOP and the HSRL extinction observations: iii) the assumed CALIOP $S_{a,532}$ value for each aerosol layer detected in the vertical could be erroneous and shows less variability than in reality. We would like to stress the potential importance of this third factor. Further investigation and validation of the CALIOP assumed $S_{a,532}$ product should be carried out on a broader scale and time

ACPD
10, 27967–28015, 2010

period (i.e. measurements of $S_{a,532}$ along the CALIOP track over a large seasonal and spatial range).

The small variation of the CALIOP $S_{a,532}$@40 km profile in Fig. 5c explains the strong resemblance of the CALIOP $\beta_{a,532}$@40 km and $\alpha_{a,532}$@40 km profiles in Fig. 5b and d. The HSRL $\alpha_{a,532}$ profile in Fig. 5d clearly shows an increase in the extinction coefficient values between 2.4 and 3 km, followed by a stronger peak extending from ~2 km down to a few hundred meters close to the ground. On the other hand, the CALIOP $\alpha_{a,532}$@40 km profile reports the uppermost increase higher than for the HSRL with an approximate difference of 500 m on the vertical and seems to pick up ~500 m of the lowest aerosol peak (between 1.4 and 1.9 km).

To summarize, there are several important dissimilarities between the CALIOP and the HSRL extinction coefficient profiles on 4 August 2007. The potential reasons for those discrepancies are investigated in the remainder of this study.

4.3.1 CALIOP's failed detection of tenuous aerosol layers and its signal not reaching down to the ground

We attempt to estimate the impact of failed detection of low-level aerosol layers due to high signal attenuation on column AOD, using the collocated HSRL $\alpha_{a,532}$ profile of Fig. 5d (red). The integration of the HSRL $\alpha_{a,532}$ profile from the ground to the base of the lowest layer detected by CALIOP (leading to an AOD of 0.23 from a few hundred meters to 1.5 km), and again beginning above the top of the highest layer detected by CALIOP (AOD of 0.01 from 3 km to the top) adds a total of 0.24 to the standard CALIOP AOD of 0.32. Another option is to use the collocated HSRL layer aerosol optical thickness parameter, AOD^{L}_{532} (Table 2) instead of the HSRL $\alpha_{a,532}$ profile, as AOD^{L}_{532} is reported from further down close to the ground (~60 m), using the molecular channel. The HSRL AOD^{L}_{532} reports a slightly higher AOD value of 0.26 from the ground up to the lowest layer detected by CALIOP (1.5 km), adding a total of 0.27 to the standard CALIOP AOD. This would, at least, account for the amount of extinction

ACPD
10, 27967–28015, 2010

needed for CALIOP to be consistent with the AERONET AOD range 1/2 h around the overpass (0.48 to 0.73) on 4 August 2007. Based on the comparisons shown in Fig. 1, we speculate that this is not a problem specific to this case. Indeed, the CALIOP team has developed an alternative retrieval philosophy for low-lying aerosol layers. In those cases where transparent aerosol layers are detected, if (a) the initial estimate of layer base is "close to" the Earth's surface, and (b) the surface is reliably detected, and (c) the mean attenuated backscatter between the initial base estimate and the surface is positive, the layer base estimate is revised downward to a new, lower altitude very near the surface. This new scheme has been implemented in version 3 data products, and preliminary results suggest that it will have the desired effects (Vaughan et al., 2010).

4.3.2 CALIOP's potentially erroneous assumed lidar extinction-to-backscatter ratio value per detected aerosol layer

An alternative CALIOP $\alpha_{a,532}$@40 km* profile was computed by applying a newly devised extinction retrieval to all previously cloud-screened CALIOP β'_{532}@1/3 km profiles in the 40 km region of interest (such as shown on Fig. 4b with a ~4/3 km horizontal resolution). The alternative extinction retrieval uses a simple iterative numerical method, starting from a height z_0 (here, ~4 km) down to the ground. The aerosol extinction coefficient is assumed equal to zero at height z_0, the molecular extinction and backscatter coefficient profiles are taken from the GEOS-5 model provided in the CALIOP level 1 data, and the $S_{a,532}$ profile is taken from the closest HSRL profile to CATZ-Sanders (Fig. 5c, red). Additional information on the alternative extinction retrieval is given in the Appendix A. The alternative CALIOP AOD values along the 40 km segment are then obtained by integrating each alternative extinction coefficient profile in the "curtain scene" between ~1.4 km and ~3.2 km, range of CALIOP detected aerosol layers and extent of the standard CALIOP $\alpha_{a,532}$@40 km profile on Fig. 5d (black). The result is a 40 km-averaged alternative CALIOP AOD value of 0.44 compared to the standard CALIOP AOD value of 0.32 close to CATZ-Sanders on 4 August 2007 (Fig. 3b). It ap-

ACPD
10, 27967–28015, 2010

pears that, in this case study, modifying the extinction-to-backscatter lidar ratio profile in the CALIOP extinction retrieval has less of an effect on the final AOD retrieval (adds 0.12 in the AOD) than the impact of failed detection of low-level aerosol layers due to high signal attenuation (adds 0.27 in the AOD, previous section). The conclusion of a minor impact of CALIOP's potentially erroneous assumed S_a value compared to the inability of its signal to reach all the way down to the surface on the AOD retrieval can not yet be stated in a general context. This result may, indeed, be strongly influenced by very similar averaged HSRL and CALIOP S_a values (Fig. 5c) on 04 August 2007 close to CATZ-Sanders.

4.3.3 CALIOP's cloud clearing, averaging and calibration of the attenuated backscatter coefficient profile

Figure 6 shows the closest HSRL β'_{532}profile (red) to CATZ-Sanders on 04 August 2007, along with three alternative CALIOP β'_{532} profiles. The first one, called $\beta'^{C}_{532,\mathrm{ncs}}$@40 km* (in blue on Fig. 6), is obtained by applying a sliding average of four β'_{532}@1/3 km profiles before averaging all valid profiles in the 40 km segment close to CATZ-Sanders (white line on Fig. 3a). The second one, called $\beta'^{C}_{532,\mathrm{cs}}$@40 km* (in green on Fig. 6), corresponds to the first one, but with a sliding average of four profiles on the cloud-screened β'_{532}@1/3 km "curtain scene" (Fig. 4b).

We note that the first two alternative CALIOP profiles (blue and green, Fig. 6) show more general variability than the HSRL β'^{H}_{532} profile (red, Fig. 6), illustrating the differences in SNR between the two instruments, and emphasizing the utility of using a broader horizontal averaging scale of 80 km as the input of CALIOP's standard multi-scale averaging engine and feature detection algorithm. In addition, the comparison between CALIOP $\beta'^{C}_{532,\mathrm{ncs}}$@40 km* (blue) and $\beta'^{C}_{532,\mathrm{cs}}$@40 km* (green) confirms the presence of a reported cloud in the 40 km of interest around 2.2 km in height, that could lead to an erroneous aerosol layer classification and corresponding S_a value in

ACPD
10, 27967–28015, 2010

the level 2 extinction retrieval algorithm.

Two major factors need to be considered when comparing the HSRL β'^{H}_{532}(red) and the CALIOP $\beta'^{C}_{532,cs}$@40 km* (green) profiles. First of all, the instruments differ regarding their calibration technique and accuracy. The accuracy of the CALIOP level 1 products (and, by consequence, many of the level 2 products) critically depends on the accuracy of the calibration of the attenuated backscatter profiles. The nighttime CALIOP 532 nm parallel attenuated backscatter measurement is calibrated by determining the ratio between the measured signal and the total backscatter estimated from an atmospheric scattering model (Powell et al., 2009; Hostetler et al., 2006; Russell et al., 1979) across a range altitude of 30–34 km, where aerosol loading is assumed to be low and there is still sufficient molecular backscatter to produce a robust signal. Because of the degradation of the SNR in the calibration region due to noise associated with solar background signals, the CALIOP daytime 532 nm calibration coefficients are interpolated from the adjacent nighttime data segments (Powell et al., 2010). On the other hand, the Airborne HSRL is internally calibrated to a high accuracy (~1–2%), and does not rely on normalization to estimated backscatter from assumed clear-air regions for calibration (Hair et al., 2008).

Secondly, the HSRL β'^{H}_{532} (red) and CALIOP $\beta'^{C}_{532,cs}$@40 km* (green) profiles differ in terms of the atmospheric attenuation of each lidar signal. The attenuation of the CALIOP profile is measured relative to the base of CALIOP's molecular normalization region at 30-km (the minimal beam attenuation above this region is included in the calibration coefficient). Because the HSRL is internally calibrated, and does not rely on molecular normalization, atmospheric attenuation of the HSRL signal is measured relative to a point 1.5 km below the aircraft, z_{HSRL} (~7.5 km).

ACPD
10, 27967–28015, 2010

For those cases where there are no clouds above the HSRL, the magnitudes of the attenuated backscatter profiles measured by the two instruments will differ by a factor of

$$\Delta T^2 = \exp\left(-2\int_{30\,\mathrm{km}}^{z_{\mathrm{HSRL}}}\left(\alpha_m(z)+\alpha_{O_3}(z)\right)dz\right) \quad (3)$$

so that

$$\beta'^{C}_{532,\mathrm{cs}}@40\mathrm{km}^*(z) = \Delta T^2 \beta'^{H}_{532}(z) \quad (4)$$

Aerosol loading is considered negligible between 30-km and z_{HSRL}, and thus no aerosol attenuation term is included in the calculation of ΔT^2. The requisite values for $\alpha_{O_3}(z)$ and $\alpha_m(z)$ are estimated using the gridded ozone and molecular number density profile data from the GEOS-5 analysis product available from the NASA Goddard Global Modeling and Assimilation Office (GMAO).

ΔT^2 for the $\beta'^{C}_{532,\mathrm{cs}}@40\,\mathrm{km}^*$ profile of Fig. 6 is 0.88 (molecular and ozone optical depth are respectively ~0.04 and ~0.02). Hence, if the CALIOP signal was correctly calibrated, HSRL β'^{H}_{532} (red) would be ~12% higher than the CALIOP $\beta'^{C}_{532,\mathrm{cs}}@40\,\mathrm{km}^*$ (green) profile. Figure 6 shows, in fact, a general overestimation of the HSRL β'^{H}_{532} profile (red), especially along the uppermost and lowest intensity peak. We have computed the difference between the integrated red and green profiles of Fig. 6 as follows:

$$\left[\int_{z=0\mathrm{km}}^{z=z_{\mathrm{HSRL}}}\beta'^{H}_{532}dz - \int_{z=0\mathrm{km}}^{z_{\mathrm{HSRL}}}\beta'^{C}_{532,\mathrm{cs}}@40\mathrm{km}^*dz\right]\times 100 \div \int_{z=0\mathrm{km}}^{z_{\mathrm{HSRL}}}\beta'^{H}_{532}dz = 13.74\% \quad (5)$$

The amount of overestimation of the integrated HSRL β'^{H}_{532}on the integrated CALIOP $\beta'^{C}_{532,\mathrm{cs}}@40\,\mathrm{km}^*$ profile is similar to what would be expected in the case of a correctly calibrated CALIOP signal on 04 August 2007 near CATZ-Sanders. Nonetheless, (Powell et al., 2010 and Rogers et al., 2010) show that, in general, the CALIOP calibration remains an issue in the version 2 level 1 attenuated backscatter products. Indeed,

ACPD
10, 27967–28015, 2010

(Powell et al., 2010) revealed that the use of a constant scaling factor to transfer calibration from nighttime to daytime measurements in the version 2 data products was precluded by thermally-induced misalignment of the transmitter and receiver, causing the daytime signal levels to vary non-linearly. In conclusion, the sub-optimal Version 2 daytime calibration of CALIOP's raw signal can be added as a fourth potential reason for discrepancies between CALIOP and either HSRL or MODIS. The next Version 3 CALIOP data release improves upon this calibration scheme with significant modifications (Powell et al., 2010).

As a result of the different signal attenuation, in order to rigorously compare the CALIOP and HSRL total attenuated backscatter coefficients we needed to normalize the CALIOP profile ($\beta'^{C}_{532,cs}$@40 km**, in black on Fig. 6) using the ratio of the mean $\overline{\beta'^{H}_{532}}$ by the mean $\overline{\beta'^{C}_{532,cs}-40\text{km}^{*}}$ in a "clear air" region (from 4.5 to 7.5 km). The normalized CALIOP $\beta'^{C}_{532,cs}$@40 km** (black, Fig. 6) is fairly close to the HSRL β'^{H}_{532} profile (red, Fig. 6) with ~93% of the differences between both profiles below $0.5\times10^{-3}\,\text{km}^{-1}\,\text{sr}^{-1}$. The integration of both profiles on the vertical is within 1% of each other.

We note that the normalized CALIOP $\beta'^{C}_{532,cs}$@40 km** (black) and the HSRL β'^{H}_{532} profile (red) should show the same trend, given that both instruments are sampling the same aerosol layer at the same wavelength. Both profiles decrease rapidly with altitude at heights below ~1.9 km, most probably due to strong aerosol attenuation. The HSRL backscatter and extinction profiles corresponding to the β'^{H}_{532} profile (red) are measured directly while the CALIOP backscatter and extinction profiles corresponding to $\beta'^{C}_{532,cs}$@40 km**(black) are only retrieved in those regions where an aerosol layer is identified. The strong aerosol attenuation of the signal below ~1.9 km in Fig. 6, together with the additional noise that CALIOP has to take into account, is what causes the CALIOP layer detection algorithm to fail to identify the full vertical extent of the layer. This leads to a premature CALIOP apparent aerosol base height determination explaining the lack of aerosol reported below ~1.4 km in Fig. 5b.

ACPD
10, 27967–28015, 2010

Figure 7 shows the comparison of the collocated HSRL (red, Fig. 6) and CALIOP (black, Fig. 6) total attenuated backscatter coefficients from ~8 km down to the surface close to CATZ-Sanders on 4 August 2007.

According to Fig. 7, a large number of collocated HSRL β'^{H}_{532} and CALIOP $\beta'^{C}_{532,cs}$@40 km** coefficients are below 1.5×10^{-3} km^{-1} sr^{-1} (57%). CALIOP shows a fairly similar amount of those lower values of HSRL total attenuated backscatter coefficients under and above the one-to-one line with a comparable mean value of 8–9 $\times 10^{-4}$ km^{-1} sr^{-1}. On the other hand, the overall regression line on Fig. 7 (red line) shows a slight CALIOP overestimation of the HSRL total attenuated backscatter coefficients. Nonetheless, constraining the averaging, the cloud screening and the normalization of the CALIOP level 1 attenuated backscatter measurements shows good agreement with the HSRL β'^{H}_{532} profile (correlation coefficient of 0.91, insignificant offset and a slope very close to 1).

5 Conclusions

While first attempting to assess the general consistency between both space-borne CALIOP column integrated aerosol extinction profiles and MODIS AOD retrievals, we have shown low correlation ($R \sim 0.4$) and a general underestimation (by 66%) of the MODIS-derived AOD by CALIOP (version 2) during Summer 2007 over the Eastern part of the United States. The possible reasons for such discrepancies between both satellite retrievals are discussed and explored based on a carefully selected case study containing detailed multi-sensor, multi-platform aerosol observations (ground-based AERONET sunphotometer, airborne HSRL lidar and spaceborne PARASOL, MODIS and CALIOP). The case study, part of the CATZ field campaign on 04 August 2007 over Maryland, provides detailed CALIOP suborbital observations, and in particular, the coincident airborne HSRL instrument to illustrate what are likely to be the most important potential reasons for the overall bias in the CALIOP version 2 AOD:

ACPD
10, 27967–28015, 2010

(i) CALIOP's low SNR prevents the detection of tenuous aerosol layers. Furthermore, as shown above, the attenuation of the signal by dense aerosol plumes can drive the signal within a layer below CALIOP's detection threshold, and thus prevents identification of the full vertical extent of the layer. This explains the lack of CALIOP $\beta_{a,532}$@40 km data below ~1.4 km and the premature determination of the aerosol layer base on 04 August 2007 near CATZ-Sanders. Using the collocated HSRL layer AOD above and below the CALIOP detected aerosol layer altitudes adds a total of 0.27 to the CALIOP AOD value.

(ii) The assumed CALIOP $S_{a,532}$@40 km profile could be biased and the true, continuous variability of $S_{a,532}$ found in nature may not be properly represented by the assumed CALIOP $S_{a,532}$ values underlying the aerosol retrieval algorithm. Applying an alternative extinction retrieval to the CALIOP attenuated backscatter profiles using the independently measured HSRL lidar ratio profile on 04 August 2007 near CATZ-Sanders adds ~0.1 to the total CALIOP AOD.

(iii) There is a significant bug in the version 2 cloud-screening algorithm. This presumably explains the disparity between CALIOP and HSRL measured total attenuated backscatter coefficient, and in consequence, retrieved aerosol backscatter and extinction coefficient profiles around 2.2 km near CATZ-Sanders on 4 August 2007. The cloud contamination has the opposite effect of artificially increasing the AOD value in the general underestimation of the CALIOP AOD.

(iv) Finally, although the CALIOP signal seemed to be fairly well calibrated during our case study of 04 August 2007 near CATZ-Sanders, it is important to mention that the version 2 CALIOP daytime calibration scheme has proven to be suboptimal, leading to bias errors in the 532 nm total attenuated backscatter and, in consequence, will propagate into the CALIOP aerosol extinction products (Rogers et al., 2010; Powell et al., 2010)

Let us mention that multiple scattering, which is assumed to be negligible in the CALIOP level 2 aerosol algorithms could also be a potential reason for the

ACPD
10, 27967–28015, 2010

extinction retrieval errors. Indeed, multiple scattering effects are more significant in the case of spaceborne than airborne lidar systems due to a larger footprint. They can alter the apparent extinction or transmittance of the medium, lead to depolarization of the returned signal, and can produce stretching of the return pulse. Nevertheless, the effects of multiple scattering seem to apply mostly in the case of dense dust plumes recording high AOD values. Based on Winker et al. (2003), in the case of aerosols other than large dust particles, multiple scattering is likely to contribute, at best, in a 10% correction in the retrieval of aerosol extinction profiles. In this case, the error introduced by ignoring multiple scattering effects is negligible compared to a fractional error of 30% in the lidar S_a ratio (resulting in an AOD fractional error of ~50% when the AOD is around 0.5). In the case of fresh, dense dust layers close to the source region, the analysis of airborne in situ size distribution observations during SAMUM-1 (Saharan Mineral Dust Experiment, Southern Morocco, May–June 2006) have shown that the multiple-scattering-related underestimation of the extinction coefficient in the CALIOP lidar signals ranges from 10%–40% (Wandinger et al., 2010). On another hand, Liu et al. (2010) shows that for moderately dense dust cases (AOD~1 and extinction smaller than 1 km^{-1}), the vertical homogeneity of the particulate depolarization ratio profile indicates negligible impact from multiple scattering. Multiple scattering effects are not considered in our paper as all the AOD observations during our case study of 04 August 2007 are below 1 (Fig. 3) and less than 1% of the matching MODIS-CALIOP AOD values present a CALIOP AOD above 1 (Fig. 1b).

In conclusion, this study has helped illustrate a few potential reasons for deficiencies in the Version 2 level 2 aerosol extinction product. We hope that our study will improve the understanding of the results obtained in previous studies that have used CALIOP version 2 data. The next version of CALIOP data (version 3) is currently being processed and will include corrections to many of the factors described above. The impact of such corrections on the accuracy of the Version 3

ACPD
10, 27967–28015, 2010

CALIOP extinction product will be the subject of future studies.

Appendix A

Alternative CALIOP extinction retrieval

The alternative CALIOP extinction retrieval is based on a simple numerical integration technique. Let us define:

0: the height of the CALIOP LIDAR,

0-z_0: the height range where there are no aerosols and

z: the height of the scattering aerosol layer.

The LIDAR signal, $P(z)$, can be written as follows:

$$P(z) = \frac{K}{z^2} \times \beta(z) \times T(0,z)^2 = \frac{K}{z^2} \times \beta(z) \times T(0,z_0)^2 \times T(z_0,z)^2, \quad \text{(A1)}$$

where K = the system constant, z = the range, $\beta(z)$ = the total backscatter coefficient profile and $T(z)^2$ = the atmospheric two-way transmittance (i.e. the signal attenuation).

The total attenuated backscatter coefficient profile, $\beta'(z)$, can be written as follows:

$$\beta'(z) = \beta(z) \times T(z_0,z)^2 \quad \text{(A2)}$$

Substituting Eq. (A2) in Eq. (A1) leads to:

$$P(z) = \frac{K}{z^2} \times \beta'(z) \times T(0,z_0)^2 \quad \text{(A3)}$$

The combination of Eqs. (A1) and (A3) leads to:

$$\beta(z) \times T(0,z)^2 = \beta'(z) \times T(0,z_0)^2 \quad \text{(A4)}$$

ACPD
10, 27967–28015, 2010

with:

$$T(0,z)^2 = \exp\left[-2\int_0^z (\alpha_a(z) + \alpha_m(z))dz\right] \quad \text{(A5)}$$

$$T(0,z_0)^2 = \exp\left[-2\int_0^{z_0} \alpha_m(z)dz\right] \quad \text{(A6)}$$

$$\beta(z) = \beta_a(z) + \beta_m(z) \quad \text{(A7)}$$

$$S_a(z) = \frac{\beta_a(z)}{\alpha_a(z)} \quad \text{(A8)}$$

where $\alpha_a(z)$ and $\alpha_m(z)$ are the aerosol and molecular extinction coefficient profiles, $\beta_a(z)$ and $\beta_m(z)$ are the aerosol and molecular backscatter coefficient profiles and $S_a(z)$ is the extinction-to-backscatter lidar ratio.

Substituting Eqs. (A5–A8) in Eq. (A4) leads to:

$$\alpha_a(z) = S_a(z) \times \left(\beta'(z)\exp\left[2\int_{z_0}^z (\alpha_a(z) + \alpha_m(z))dz\right] - \beta_m(z)\right) \quad \text{(A9)}$$

Let us write Eq. (A9) replacing the integral by a discrete sum over different layers i in the vertical:

$$\alpha_a(z_i) = S_a(z_i) \times \left(\beta'(z_i)\exp\left[2\sum_{k=0}^{i-1} (\alpha_a(z_k) + \alpha_m(z_k))\Delta z\right] - \beta_m(z_i)\right) \quad \text{(A10)}$$

$\alpha_a(z_i)$ can then be computed using $S_a(z_i)$ from the collocated HSRL instrument, $\beta'(z_i)$ from the CALIOP β'_{532} @ 1/3 km profile product (cloud-screened with the CALIOP

ACPD
10, 27967–28015, 2010

cloud@1/3 km product), $\beta_m(z_i)$ and $\alpha_m(z_i)$ from the gridded molecular number density profile data from the GEOS-5 analysis product available from the NASA Goddard Global Modeling and Assimilation Office (GMAO) and knowing Δz, the thickness of each layer i on the vertical.

According to Eq. (A10), the aerosol extinction coefficient α_a at height z_1 (first layer below z_0, where aerosol load is supposed negligible) can be computed as follows:

$$\alpha_a(z_1) = S_a(z_1) \times \left(\beta'(z_1)\exp\left[2\alpha_m(z_0)\Delta z\right] - \beta_m(z_1)\right) \quad \text{(A11)}$$

Acknowledgements. The authors gratefully acknowledge the NOAA Air Resources Laboratory (ARL) for the provision of the HYSPLIT transport and dispersion model and/or READY website (http://www.arl.noaa.gov/ready.php) used in this publication. They also thank the AERONET network (especially Thomas Eck), the NASA HSRL, CALIPSO and MODIS team (especially Robert Levy) and the CNES POLDER team for their data. A special acknowledgment goes towards the UMBC lidar team and the Sunphotometer/Satellite group at NASA AMES Research Center. This research was supported by an appointment to the NASA Postdoctoral Program at the Ames Research Center, administered by Oak Ridge.

References

Anderson, T. L., Robert, J., Charlson R. J., David, M., Winker D. M., John, A., Ogren, J. A., Holmén, K.: Mesoscale Variations of Tropospheric Aerosols, J. Atmos. Sci., 60(1), 119–136, 2003.

Cattrall, C., Reagan, J., Thome, K., and Dubovik, O.: Variability of aerosol and spectral lidar and backscatter and extinction ratios of key aerosol types derived from selected Aerosol Robotic Network locations, J. Geophys. Res., 110, D10S11, doi:10.1029/2004JD005124, 2005.

Chu D. A., Kaufman, Y. J., Ichoku, C., Remer, L. A., Tanré, D., and Holben, B. N.: Validation of MODIS aerosol optical depth retrieval over land, J. Geophys. Res., 29(12), doi:10.1029/2001GL013205, 2002.

ACPD

10, 27967–28015, 2010

Deuzé, J.-L., Bréon, F.-M., Devaux, C., Goloub, P., Herman, M., Lafrance, B., Maignan, F., Marchand, A., Nadal, F., Perry, G., and Tanré, D.: Remote sensing of aerosols over land-surfaces from POLDER-ADEOS-1 polarized measurements, J. Geophys. Res., 106, 4913–4926, 2001.

Draxler, R. R. and Rolph, G. D.: HYSPLIT (HYbrid Single-Particle Lagrangian Integrated Trajectory) Model access via NOAA ARL READY Website (http://ready.arl.noaa.gov/HYSPLIT.php), NOAA Air Resources Laboratory, Silver Spring, MD, 2010.

Dubovik, O. and King, M. D.: A flexible inversion algorithm for retrieval of aerosol optical properties from Sun and sky radiance measurements, J. Geophys. Res., 105, 20673–20696, 2000a.

Dubovik, O., A. Smirnov, Smirnov A., Holben B. N., King M. D., et al.: Accuracy assessments of aerosol optical properties retrieved from Aerosol Robotic Network (AERONET) Sun and Sky radiance measurements, J. Geophys. Res., 105(D8), 9791–9806, 2000b.

Eck, T. F., Holben, B. N., Reid, J. S., Dubovik, O., Smirnov, A., O'Neill, N. T., Slutsker, I., and Kinne, S.: Wavelength dependence of the optical depth of biomass burning, urban and desert dust aerosols, J. Geophys. Res., 104, 3133–31350, 1999.

Gonzi, S. and Palmer, P. I.: Vertical transport of surface fire emissions observed from space, J. Geophys. Res., 115, D02306, doi:10.1029/2009JD012053, 2010.

Hair, J. W., Caldwell, L. M., Krueger, D. A., and She, C. Y.: High-spectral-resolution lidar with iodine-vapor filters: measurement of atmospheric-state and aerosol profiles, Appl. Optics, 40, 5280–5294, 2001.

Hair, J. W., Hostetler, C. A., Cook, A. L., Harper, D. B., Ferrare, R. A., Mack, T. L., Welch, W., Isquierdo, L. R., and Hovis, F. E.: Airborne high spectral resolution lidar for profiling aerosol optical properties, Appl. Optics, 47, 6734–6752, doi:10.1364/AO.47.006734, 2008.

Holben, B. N., Eck, T. F., Slutsker, I., Tanré, D., Buis, J. P., Setzer, A., Vermote, E., Reagan, J. A., Kaufman, Y. J., Nakajima, T., Lavenu, F., Jankowiak, I., and Smirnov, A.: AERONET-A federated instrument network and data archive for aerosol characterization, Remote Sens. Environ., 66, 1–16, 1998.

Hostetler, C. A., Liu, Z., Reagan, J., Vaughan,M., Winker, D., Osborn, M., Hunt, W. H., Powell, K. A., and Trepte, C.: CALIOP Algorithm Theoretical Basis Document, Calibration and level 1 Data Products, PC-SCI-201, NASA Langley Research Center, Hampton, VA 23681 (available online at: http://www-calipso.larc.nasa.gov/resources/project_documentation.php), 2006.

ACPD
10, 27967–28015, 2010

Jones, T. A. and Christopher, S. A.: Statistical properties of aerosol-cloud-precipitation interactions in South America, Atmos. Chem. Phys., 10, 2287–2305, doi:10.5194/acp-10-2287-2010, 2010.

Kaufman, Y. J. and Tanré, D.: Algorithm for remote sensing of tropospheric aerosol from MODIS, Product ID: MOD04, 85 pp., 1998.

Kendall, M. G. and Maurice, G.: A Course in Multivariate Analysis, London: Charles W. Griffin & Co., Ltd., 1957.

Kim, S.-W., Berthier, S., Raut, J.-C., Chazette, P., Dulac, F., and Yoon, S.-C.: Validation of aerosol and cloud layer structures from the space-borne lidar CALIOP using a ground-based lidar in Seoul, Korea, Atmos. Chem. Phys., 8, 3705–3720, doi:10.5194/acp-8-3705-2008, 2008.

Kittaka, C., Winker, D., Omar, A., Liu, Z., Vaughan, M., and Trepte, C.: Global Aerosol Distributions Derived From the CALIPSO Observations, Eos Trans. AGU, 89(53), Fall Meet. Suppl., Abstract A41A–0078, 2008.

Kuhlmann, J. and Quaas, J.: How can aerosols affect the Asian summer monsoon? Assessment during three consecutive pre-monsoon seasons from CALIPSO satellite data, Atmos. Chem. Phys., 10, 4673–4688, doi:10.5194/acp-10-4673-2010, 2010.

Levy, R. C., Remer, L. A., Kleidman, R. G., Mattoo, S., Ichoku, C., Kahn, R., and Eck, T. F.: Global evaluation of the Collection 5 MODIS dark-target aerosol products over land, Atmos. Chem. Phys., 10, 10399–10420, doi:10.5194/acp-10-10399-2010, 2010.

Liu, Z., Vaughan, M. A., Winker, D. M., Kittaka, C., Kuehn, R. E., Getzewich, B. J., Trepte, C. R., and Hostetler, C. A.: The CALIPSO Lidar Cloud and Aerosol Discrimination: Version 2 Algorithm and Initial Assessment of Performance, J. Atmos. Ocean. Tech., 26, 1198–1213, doi:10.1175/2009JTECHA1229.1, 2009

Liu, Z., Winker D. M., Omar A. H., et al.: Effective lidar ratios of dense dust layers over North Africa derived from the CALIOP measurements, J. Quant. Spectrosc. RA., doi:10.1016/j.jqsrt.2010.05.006, in press, 2010.

Mamouri, R. E., Amiridis, V., Papayannis, A., Giannakaki, E., Tsaknakis, G., and Balis, D. S.: Validation of CALIPSO space-borne-derived attenuated backscatter coefficient profiles using a ground-based lidar in Athens, Greece, Atmos. Meas. Tech., 2, 513–522, doi:10.5194/amt-2-513-2009, 2009.

ACPD

10, 27967–28015, 2010

McGill, M. J., Hlavka, D. L., Hart, W. D., Welton, E. J., and Campbell, J. R.: Airborne lidar measurements of aerosol optical properties during SAFARI-2000, J. Geophys. Res., 108(D13), 8493, doi:10.1029/2002JD002370, 2003.

McGill, M. J., Vaughan, M. A., Trepte, C. R., Hart, W. D., Hlavka, D. L., Winker, D. M., and Kuehn, R.: Airborne validation of spatial properties measured by the CALIPSO lidar, J. Geophys. Res., 112, D20201, doi:10.1029/2007JD008768, 2007.

McMillan, W. W., Pierce R. B., Sparling L. C., et al.: An observational and modeling strategy to investigate the impact of remote sources on local air quality: A Houston, Texas, case study from the Second Texas Air Quality Study (TexAQS II), J. Geophys. Res., 115, D01301, doi:10.1029/2009JD011973, 2010.

Mona, L., Pappalardo, G., Amodeo, A., D'Amico, G., Madonna, F., Boselli, A., Giunta, A., Russo, F., and Cuomo, V.: One year of CNR-IMAA multi-wavelength Raman lidar measurements in coincidence with CALIPSO overpasses: Level 1 products comparison, Atmos. Chem. Phys., 9, 7213–7228, doi:10.5194/acp-9-7213-2009, 2009.

Omar, A., Winker, D., Kittaka, C., Vaughan, M., Liu, Z., Hu, Y., Trepte, C., Rogers, R., Ferrare, R., Kuehn, R., and Hostetler, C.: The CALIPSO Automated Aerosol Classification and Lidar Ratio Selection Algorithm, J. Atmos. Ocean. Tech., 26, 1994–2014, doi:10.1175/2009JTECHA1231.1, 2009.

Pappalardo, G., Wandinger U., Mona L., et al.: EARLINET correlative measurements for CALIPSO: First intercomparison results, J. Geophys. Res., 115, D00H19, doi:10.1029/2009JD012147, 2010.

Peyridieu, S., Chédin, A., Tanré, D., Capelle, V., Pierangelo, C., Lamquin, N., and Armante, R.: Saharan dust infrared optical depth and altitude retrieved from AIRS: a focus over North Atlantic - comparison to MODIS and CALIPSO, Atmos. Chem. Phys., 10, 1953–1967, doi:10.5194/acp-10-1953-2010, 2010.

Piironen, P. and Eloranta, E. W.: Demonstration of a high-spectral-resolution lidar based on an iodine absorption filter, Opt. Lett., 19, 234–236, 1994.

Powell, K. A., Hostetler, C. A., Liu, Z., Vaughan, M. A., Kuehn, R. E., Hunt, W. H., Lee, K., Trepte, C. R., Rogers, R. R., Young, S. A., and Winker, D. M.: CALIPSO Lidar Calibration Algorithms: Part I – Nighttime 532 nm Parallel Channel and 532 nm Perpendicular Channel, J. Atmos. Ocean. Tech., 26, 2015–2033, doi:10.1175/2009-JTECHA1242.1, 2009.

Powell, K. A., Vaughan, M. A., Rogers, R. R., Kuehn, R. E., Hunt, W. H., Lee, K.-P., and Murray, T. D.: The CALIOP 532-nm Channel Daytime Calibration: Version 3 Algorithm, 25th

ACPD
10, 27967–28015, 2010

International Laser Radar Conference, 2010.
Redemann, J., Q. Zhang, B,. Schmid, P. B., Russell, J. M., Livingston, H., Jonsson, H., and Remer, L. A.: Assessment of MODIS-derived visible and near-IR aerosol optical properties and their spatial variability in the presence of mineral dust, Geophys. Res. Lett., 33, L18814, doi:10.1029/2006GL026626, 2006.
Redemann, J., Vaughan, M., Shinozuka, Y., Zhang, Q., Russell, P., Livingston, J., and Remer, L.: The combined use of MODIS, CALIPSO and OMI level 2 aerosol products for calculating direct aerosol radiative effects, presentation at the combined CALIPSO-CloudSat Science Team meeting; (available at: http://cimss.ssec.wisc.edu/calipso/meetings/cloudsat_calipso_2009/Presentations/Thur/morning/Redemann_MODIS_CALIPSO_OMI.pdf), 2009.
Rogers, R. R., Hostetler C.A., Hair J. W., Ferrare R. A., Liu Z., Obland M. D., Harper D. B., Cook A. L., Powell K. A., Vaughan M. A. and Winker D. M.: Assessment of the CALIPSO Lidar 532 nm attenuated backscatter calibration using the NASA LaRC Airborne High Spectral Resolution Lidar, Atmos. Chem. Phys., submitted, doi:10.5194/acpd-10-1-2010, 2010.
Rolph, G. D.: Real-time Environmental Applications and Display sYstem (READY) Website (http://ready.arl.noaa.gov), NOAA Air Resources Laboratory, Silver Spring, MD, 2010.
Russell, P. B., Swissler, T. J., and McCormick, M. P.: Methodology for error analysis and simulation of lidar aerosol measurements, Appl. Optics, 18, 3783–3797, 1979.
Sekiyama, T. T., Tanaka, T. Y., Shimizu, A., and Miyoshi, T.: Data assimilation of CALIPSO aerosol observations, Atmos. Chem. Phys., 10, 39–49, doi:10.5194/acp-10-39-2010, 2010.
Sharma, A. R., Shailesh Kumar Kharol1, K. V. S., Badarinath1, and Darshan Singh2: Impact of agriculture crop residue burning on atmospheric aerosol loading – a study over Punjab State, India, Ann. Geophys., 28, 367–379, 2010, http://www.ann-geophys.net/28/367/2010/.
Shinozuka, Y., Redemann, J., Livingston, J. M., Russell, P. B., Clarke, A. D., Howell, S. G., Freitag, S., O'Neill, N. T., Reid, E. A., Johnson, R., Ramachandran, S., McNaughton, C. S., Kapustin, V. N., Brekhovskikh, V., Holben, B. N., and McArthur, L. J. B.: Airborne observation of aerosol optical depth during ARCTAS: vertical profiles, inter-comparison, fine-mode fraction and horizontal variability, Atmos. Chem. Phys. Discuss., 10, 18315–18363, doi:10.5194/acpd-10-18315-2010, 2010.
Smirnov, A., Holben, B. N., Kaufman, Y. J., Dubovik, O., Eck, T. F., Slutsker, I., Pietras, C., and Halthore, R.: Optical Properties of Atmospheric Aerosol in Maritime Environments, J. Atm. Sci., 59, 501–523, 2002.

ACPD
10, 27967–28015, 2010

U.S. Environmental Protection Agency: Science Algorithms of the EPA, Models-3 Community Multiscale Air Quality (CMAQ) Modeling System, EPA/600/R- 99/030. http://www.epa.gov/asmdnerl/CMAQ/CMAQscienceDoc.html, 1999.

Vaughan, M., Powell, K., Kuehn, R., Young, S., Winker, D., Hostetler, C., Hunt, W., Liu, Z., McGill, M., and Getzewich, B.: Fully Automated Detection of Cloud and Aerosol Layers in the CALIPSO Lidar Measurements, J. Atmos. Ocean. Tech., 26, 2034–2050, doi:10.1175/2009JTECHA1228.1, 2009.

Vaughan, M., Kuehn, R., Tackett,J., Rogers, R., Liu, Z., Omar, A., Getzewich, B., Powell, K., Hu, Y., Young, S., Avery, M., Winker, D., and Trepte, C.: "Strategies for Improved CALIPSO Aerosol Optical Depth Estimates", 25th International Laser Radar Conference (ILRC), St. Petersburg, Russia, in press, 2010.

Vermeulen, A., Devaux, C., and Herman, M.: Retrieval of the scattering and microphysical properties of the aerosols from ground-based optical measurements including polarization, I. Method, Appl. Optics, 39(33), 6207–6220, 2000.

Wandinger, U., Tesche, M., Seifert, P., Ansmann, A., Müller, D., and Althausen, D.: Size matters: Influence of multiple scattering on CALIPSO light extinction profiling in desert dust, Geophys. Res. Lett., 37, L10801, doi:10.1029/2010GL042815, 2010.

Winker, D. M., Pelon, J., and McCormick, M. P.: The CALIPSO mission: Space borne Lidar for observation of aerosols and clouds, Spie. Proc. Ser., 4893, 1–11, doi:10.1117/12.466539, 2003.

Winker, D. M., Vaughan, M. A., Omar, A., Hu, Y., Powell, K. A., Liu, Z., Hunt, W. H., and Young, S. A.: Overview of the CALIPSO mission and CALIOP data processing algorithms, J. Atmos. Ocean. Tech., 26, 2310–2323, doi:10.1175/2009JTECHA1281.1, 2009.

Yost, C. R., Minnis, P., Sun-Mack, S., Nguyen, L., and Yi, Y.: Examination of CALIPSO cloud detection in broken cloud conditions using high resolution MODIS data, CloudSat Science Team Meeting, Seattle, WA, 19 August, 2008.

Young S. A.: Analysis of lidar backscatter profiles in optically thin clouds, Appl. Optics, 34, 7019–7031, 1995.

Young, S. A. and Vaughan, M. A.: The retrieval of profiles of particulate extinction from Cloud Aerosol Lidar Infrared Pathfinder Satellite Observations (CALIPSO) data: Algorithm description, J. Atmos. Ocean. Tech., 26, 1105–1119, doi:10.1175/2008 JTECHA1221.1, 2009

ACPD
10, 27967–28015, 2010

Yu, H., Chin, M., Winker, D. M., Omar, A. H., Liu, Z., Kittaka, C., and Diehl, T.: Global view of aerosol vertical distributions from CALIPSO lidar measurements and GOCART simulations: Regional and seasonal variations, J. Geophys. Res., 115, D00H30, doi:10.1029/2009JD013364, 2010.

ACPD
10, 27967–28015, 2010

Table 1. CALIOP version 2 parameters used in this study with attributed name, variable, file, level and horizontal/vertical resolution.

Name	Variable	File	Level	Resolution due to averaging	
				Horizontal	Vertical (<8 km)
β'_{532} @ 1/3 km	Total_Attenuated_Backscatter_532	CAL_LID_L1-. . . -.hdf	1	1/3 km	30 m
cloud @ 1/3 km	Layer_Top_Altitude; Layer_Base_Altitude	CAL_LID_L2_333mCLay-. . . -hdf	2	1/3 km	30 m
aerosol @ 5 km	Layer_Top_Altitude; Layer_Base_Altitude	CAL_LID_L2_05kmALay-. . . -.hdf	2	5 km	30 m
feature @ 5 km	Feature_Classification_Flags	CAL_LID_L2_VFM-...-.hdf	2	5 km	30 m
$\beta_{a,532}$ @ 40 km	Total_Backscatter_Coefficient_532	CAL_LID_L2_40kmAProCal-. . . -.hdf	2	40 km	120 m
$\alpha_{a,532}$ @ 40 km	Extinction_Coefficient_532	CAL_LID_L2_40kmAProCal-. . . -.hdf	2	40 km	120 m
$S_{a,532}$ @ 40 km	"$\alpha_{a,532}$ @ 40 km" / "$\beta_{a,532}$ @ 40 km"	None	2	40 km	120 m

ACPD
10, 27967–28015, 2010

Table 2. HSRL parameters used in this study with attributed name, variable and short description.

HSRL data (subset file: ~4/3 km horizontal and 30 m vertical resolution)		
Name	Variable	Description (at 532 nm)
β'_{532}	532_total_attn_bsc_cloud_screened	Attenuated backscatter coefficient with cloud mask applied Reported from ~60 m to ~1.5 km below the plane (~7.5 km)
$\beta_{a,532}$	532_bsc_cloud_screened	Aerosol volume backscatter coefficient with cloud mask applied Reported from ~60 m to ~0.5 km below the plane (~8.5 km)
$\alpha_{a,532}$	532_ext	Retrieved 532 nm aerosol extinction coefficient. Reported from ~360 m to ~2.5 km below the plane (~6.4 km)
$S_{a,532}$	Sa_532	Retrieved Extinction-to-backscatter ratio Reported from ~360 m to ~2.5 km below the plane (~6.4 km)
AOD_{532}	AOT_hi	Aerosol optical thickness determined from the molecular channel near the aircraft and near the surface Derived from ~60 m to ~2.5 km below the aircraft (~6.4 km)
AOD^{L}_{532}	AOT_hi_col	Layer aerosol optical thickness determined from the molecular channel near the aircraft and near the surface Derived from ~60 m to ~2.5 km below the aircraft (~6.4 km)

ACPD
10, 27967–28015, 2010

Table 3. 4 August 2007 – Distance (km) between the different measurements during the CATZ experiment; from top to bottom, the CATZ-Sanders AERONET station (white diamond, Fig. 3a), the closest point on the HSRL track to CATZ-Sanders (green line, Fig. 3a), the closest point on the CALIOP ground track to CATZ-Sanders (white line, Fig. 3a), the closest CMAQ cell to CATZ-Sanders containing a MODIS and CALIOP AOD value (red box, Fig. 3a) and the closest CMAQ cell to CATZ-Sanders containing a POLDER AOD retrieval (black box, Fig. 3a).

Distance (km)	CATZ_Sanders	Closest point on HSRL track	Closest point on CALIOP track	CMAQ cell with CALIOP/MODIS AOD
CATZ_Sanders	–	–	–	–
Closest point on HSRL track	0.940	–	–	–
Closest point on CALIOP track	0.138	0.908	–	–
CMAQ cell with CALIOP/MODIS AOD	5.809	5.315	5.680	–
CMAQ cell with POLDER AOD	17.703	17.339	17.569	12.067

ACPD
10, 27967–28015, 2010

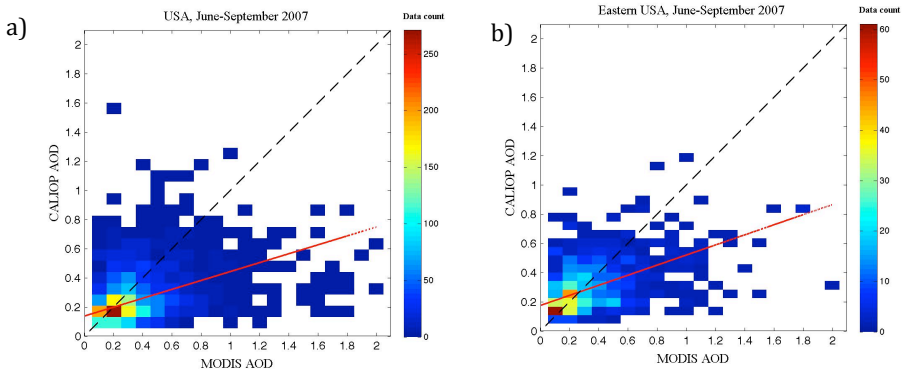

Fig. 1. Comparison between the filtered CALIOP AOD (532 nm) and MODIS AOD (550 nm) over the entire **(a)** and the Eastern (**b**, longitude > −100°) United States; only positive MODIS AOD and CALIOP $\alpha_{a,532}$@40 km values are considered. MODIS and CALIOP data are re-mapped on the 12 × 12 km CMAQ surface grid. First principal component regression method (red line) leads to $AOD_{CALIOP} = 0.31(\pm0.02)\ AOD_{MODIS} + 0.14(\pm0.01)$, $R = 0.34$, RMSD = 0.27, N = 2791 for the entire US (a) and $AOD_{CALIOP} = 0.34(\pm0.03)\ AOD_{MODIS} + 0.17(\pm0.01)$, $R = 0.43$, RMSD = 0.26, N = 807 for the Eastern US (b).

ACPD
10, 27967–28015, 2010

a)

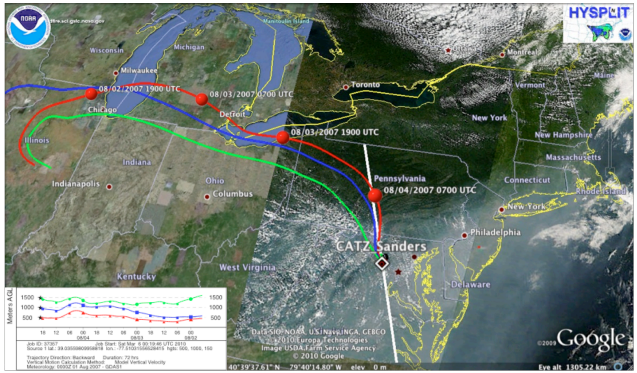

Inversion (440 nm)	Re(η)	Im(η)	ω_0	Å	τ
15:18	1.37	0.01	0.96	1.92	1.13
19:18	1.35	0.01	0.94	1.92	0.97

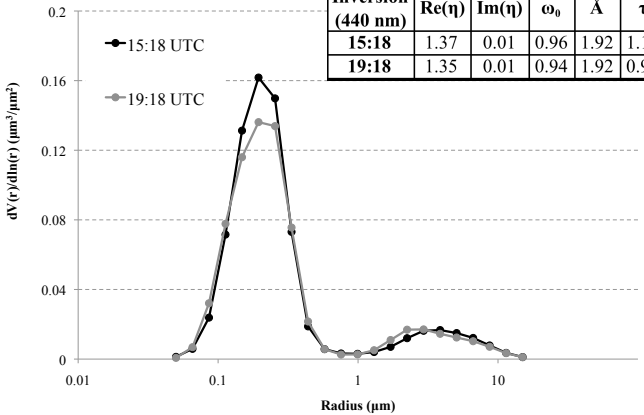

b)

Fig. 2. 4 August 2007 – **(a)** MODIS true color RGB image over the East Coast of the United States, 72 h-HYSPLIT air mass back-trajectories at 500 (red), 1000 (blue) and 1500 (green) meters above model ground level arriving at 19:00 UTC over CATZ-Sanders (white) and the CALIOP ground track (white); the back-trajectories are computed using the gridded meteorological data archives of the National Weather Service's (NWS) National Centers for Environmental Prediction (NCEP) Global Data Assimilation System (GDAS) model; **(b)** Version 2 level 1.5 CATZ-Sanders AERONET observations derived from the angular distribution of sky radiance in the almucantar (2 measurements).

ACPD
10, 27967–28015, 2010

CALIOP version 2 aerosol extinction product

M. Kacenelenbogen et al.

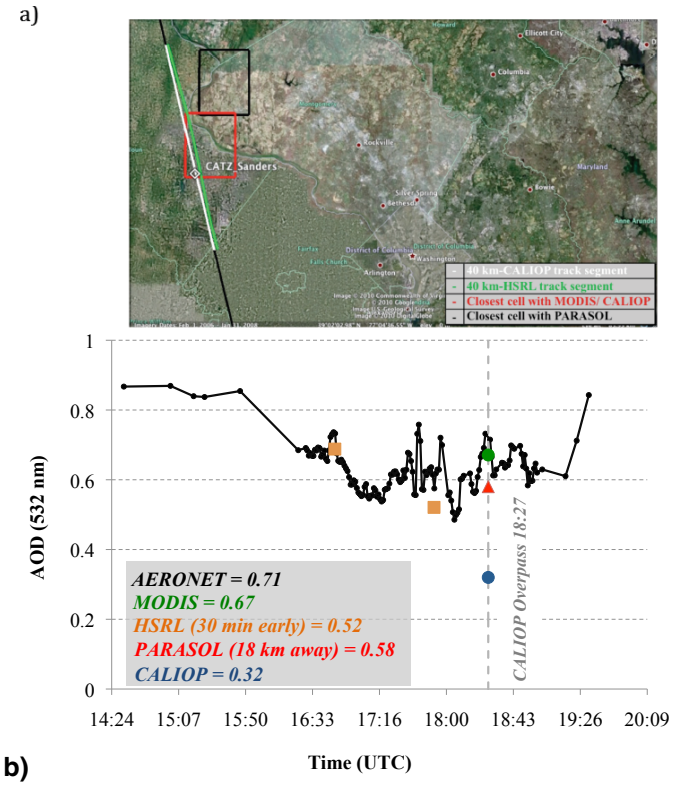

Fig. 3. 4 August 2007 – **(a)** Co-localization of CATZ-Sanders (white diamond), the closest 40 km-CALIOP track segment (white line), the corresponding closest 40 km-HSRL track segment (green line), the 12 × 12 km closest CMAQ cell (red box) reporting available MODIS and CALIOP AOD data and the closest CMAQ cell reporting available POLDER AOD data (black box); **(b)** Temporal evolution of AERONET CATZ-Sanders direct sun AOD measurements (black) and the collocated HSRL AOD retrievals during the two overpasses (AOD_{532} of Table 2, orange); At the time of the A-Train overpass (18:27 UTC, dotted grey line) over CATZ-Sanders: in green, the MODIS AOD retrieval (red box of a), in red, the POLDER AOD value (black box of a) and in blue, the CALIOP AOD value (red box of a). All AOD observations are either retrieved or computed at 532 nm (use of the Ångström exponent between 440–675 nm, 470-670 nm and 865–670 nm for AERONET, MODIS and POLDER).

ACPD
10, 27967–28015, 2010

CALIOP version 2 aerosol extinction product

M. Kacenelenbogen et al.

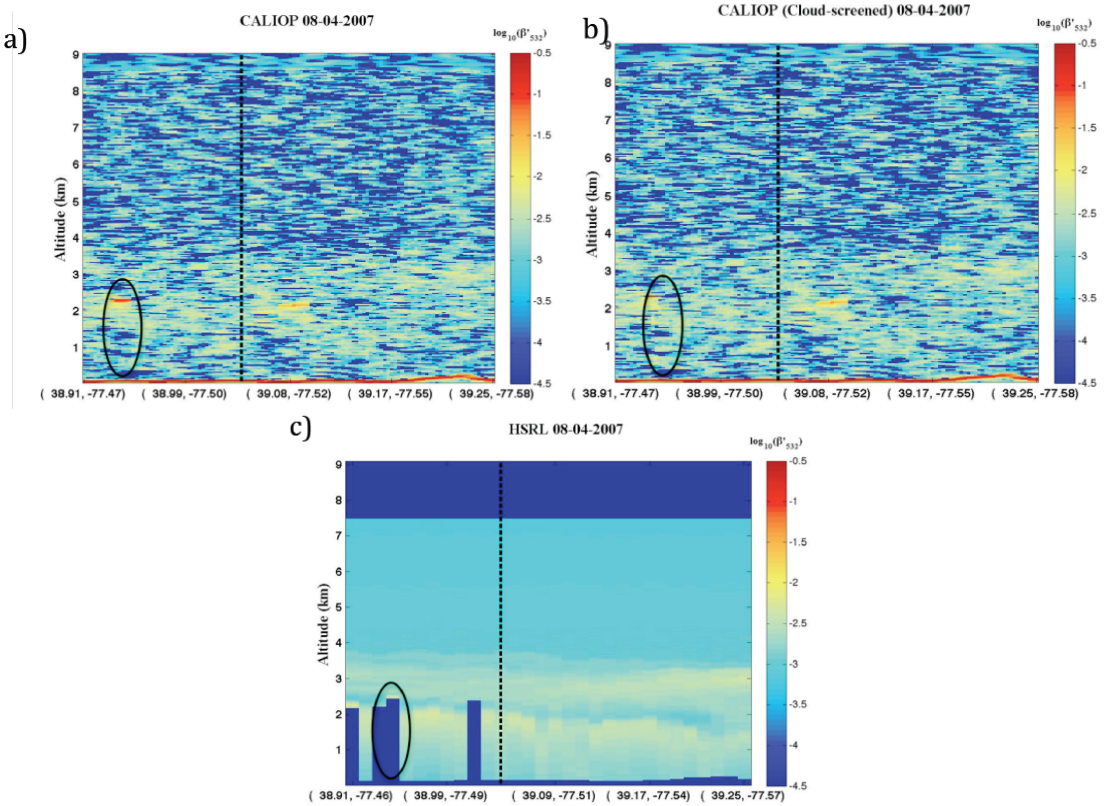

Fig. 4. 4 August 2007 – CALIOP raw **(a)**, CALIOP with further cloud-screening **(b)** and HSRL **(c)** β'_{532}"curtain scene" along the 40 km segment of its ground tracks close to CATZ-Sanders (respectively white and green line on Fig. 3a). Both CALIOP and HSRL are shown at a ~4/3 km resolution; the black circles on a, b and c point out a region with cloud contamination.

ACPD
10, 27967–28015, 2010

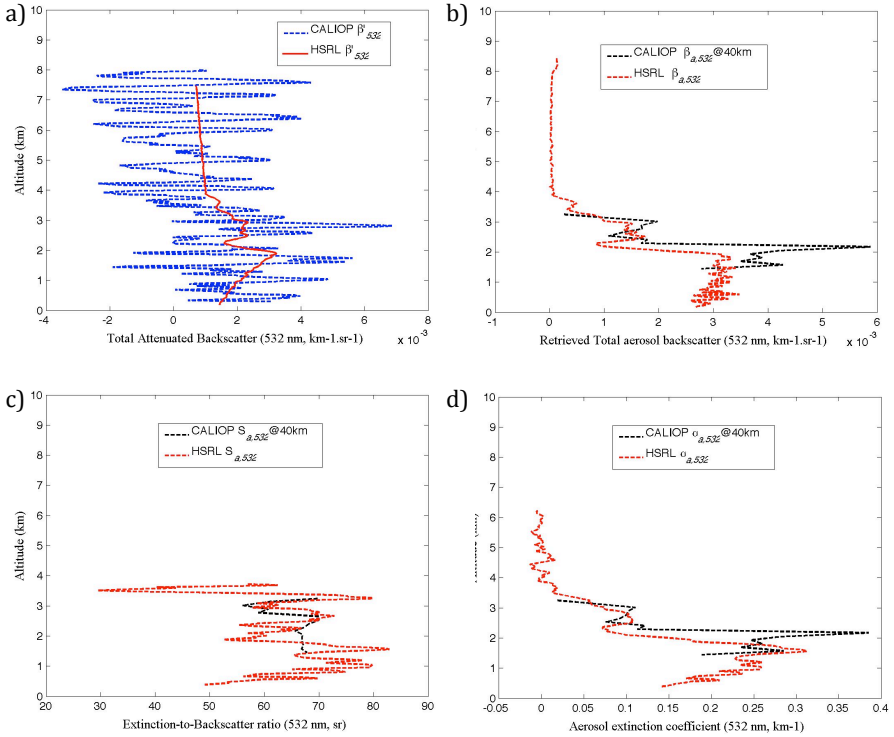

Fig. 5. 4 August 2007 – **(a)** HSRL (red) and CALIOP (blue) β'_{532} profile, both at ~4/3 km resolution; **(b)** HSRL $\beta_{a,532}$ (red) and CALIOP $\beta_{a,532}$@40 km profile (black), **(c)** HSRL $S_{a,532}$ (red) and CALIOP S_{a532}@40 km profile (black) and **(d)** HSRL $\alpha_{a,532}$ (red) and CALIOP $\alpha_{a,532}$@40 km profile (black). All profiles are the closest to CATZ-Sanders. The CALIOP and the HSRL track are ~900 m away from each other and the HSRL overpass is ~30 min early (17:52 UTC) compared to CALIOP (18:27 UTC).

ACPD
10, 27967–28015, 2010

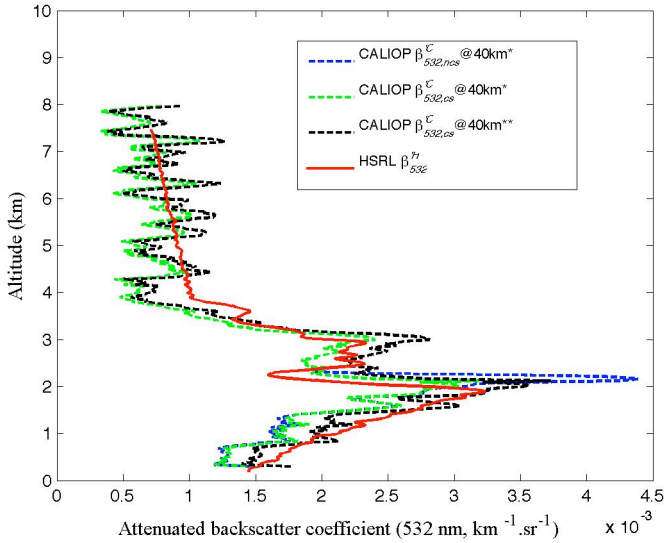

Fig. 6. 4 August 2007 – HSRL β'^{H}_{532} (red), alternative CALIOP non-cloud-screened $\beta'^{C}_{532,ncs}$@40 km** (blue), alternative CALIOP cloud-screened $\beta'^{C}_{532,cs}$@40 km* (green), and alternative CALIOP cloud-screened normalized $\beta'^{C}_{532,cs}$@40 km** profile (black); $\beta'^{C}_{532,ncs}$@40 km*, $\beta'^{C}_{532,cs}$@40 km* and $\beta'^{C}_{532,cs}$@40 km** are obtained by a sliding average of four β'_{532}@1/3 km profiles followed by averaging all valid profiles on the 40 km segment (white line on Fig. 3a); $\beta'^{C}_{532,cs}$@40 km* and $\beta'^{C}_{532,cs}$@40 km** are cloud-screened using the cloud@1/3 km product; $\beta'^{C}_{532,cs}$@40 km** is normalized by the ratio of the mean HSRL β'^{H}_{532} and the mean $\beta'^{C}_{532,cs}$@40 km* from 4.5 to 7.5 km in altitude. All profiles are collocated with CATZ-Sanders.

ACPD
10, 27967–28015, 2010

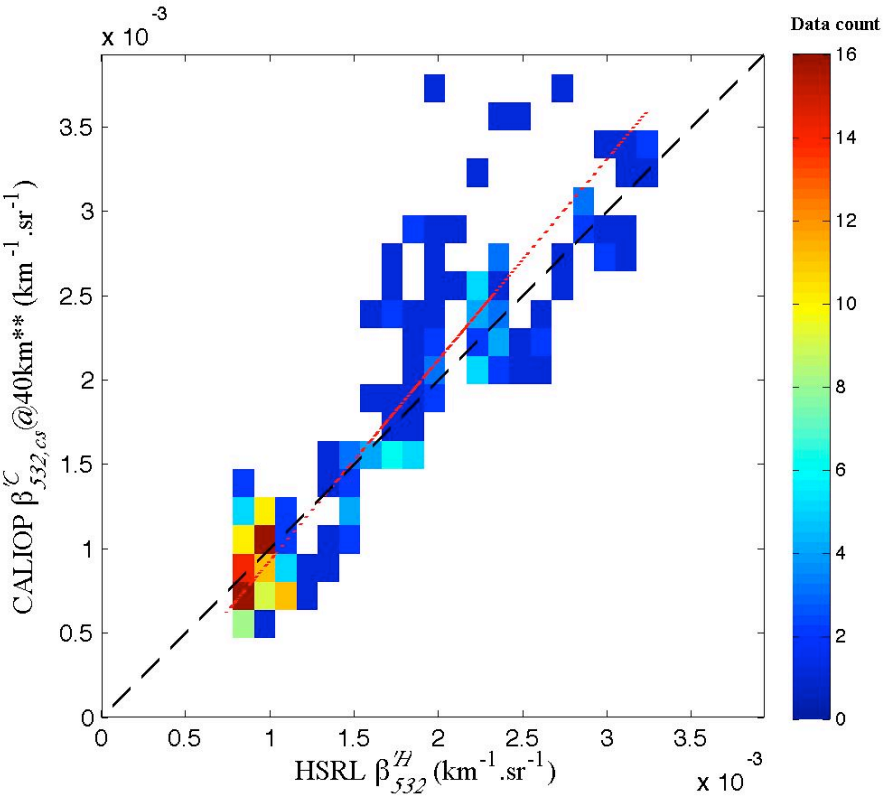

Fig. 7. 4 August 2007 – HSRL β'^{H}_{532} (red profile on Fig. 6) versus alternative cloud-screened normalized CALIOP $\beta'^{C}_{532,cs}$@40 km** (black profile on Fig. 6) coefficients from ~8 km down to the surface close to CATZ-Sanders; First principal component regression method (red line): $\beta'^{C}_{532,cs}{}^{**} = 1.19 \pm 0.03\ \beta'^{H}_{532} + 0.00 \pm 0.00$, $R = 0.91$, RMSD = 0.34 10^{-3}, N = 240.

ACPD
10, 27967–28015, 2010